7-1-1982

The atmospheric photochemical stability of CC1F2NO, CC12FNO, CC1FNO2, and CC12FNO2

George Fazekas

THE ATMOSPHERIC PHOTOCHEMICAL STABILITY OF CClF2NO, CCl2FNO, CClF2NO2 AND CCl2FNO2

GEORGE B. FAZEKAS

JULY 1982

THESIS

SUBMITTED IN PARTIAL FULFILLMENT OF THE

REQUIREMENTS FOR THE DEGREE OF MASTER OF SCIENCE

APPROVED:

Gerald A. Takacs

Project Adviser

Signature not legible

Department Head

Signature not legible

Library

Rochester Institute of Technology

Rochester, New York

Department of Chemistry

6928808

Revised sample statement for granting or denying permission to reproduce an RIT thesis.

Title of Thesis The Atmospheric Photochemical Stability of $CClF_2NO$, CCl_2FNO, $CClF_2NO_2$ and CCl_2FNO_2

I G.A. Takacs for George Fazekas hereby (grant, deny) permission to the Wallace Memorial Library, of R.I.T., to reproduce my thesis in whole or in part. Any reproduction will not be for commercial use or profit.

Or

I _____ prefer to be contacted each time a request for reproduction is made. I can be reached at the following address. _____

_____

Date Sept 21, 1983

ABSTRACT

$CClF_2NO$, $CClF_2NO$, $CClF_2NO_2$ and CCl_2FNO_2 were prepared and purified in the laboratory. Three methods for the preparation of chlorodifluoronitrosomethane were evaluated: 1) decarboxylation of the sodium salt of chlorodifluoroacetic acid in the presence of nitrosyl chloride, 2) nitrosation of chlorodifluoromethanesulfenylchoride and 3) photolysis of bromodichlorofluoromethane in the presence of nitric oxide. The vapor phase decarboxylation of the sodium salt of chlorodifluoroacetic acid in the presence of nitrosyl chloride gave chlorodifluoronitrosomethane with the highest yield and purity. Because the sodium salt of dichlofluoroacetic acid was not available to utilize in a similar manner, dichlorofluoronitrosomethane was prepared from the reaction of dichlorofluoromethanesulfenylchloride with dilute nitric acid. Chlorodifluoronitromethane and dichlorofluoronitro- methane were prepared from the oxidation of their corresponding nitroso analogs with hydrogen peroxide and characterized by their infrared spectra.

The boiling points and heats of vaporization of CCl_2FNO, $CClF_2NO$, CCl_2FNO_2 and $CClF_2NO_2$ were determined by extrapolation of their respective temperature dependent vapor pressure curves.

The UV-Vis absorption cross-sections of gaseous CCl_2FNO, $CClF_2NO$, $CFCl_2NO_2$ and CF_2ClNO_2 were investigated in order to estimate their atmospheric photochemical stability. A literature search revealed that the absorption cross-sections of these compounds had not been investigated prior to this work.

THE ATMOSPHERIC PHOTOCHEMICAL STABILITY

OF CC1F2NO, CC12FNO, CC1F2NO2 and CCL2FNO2

TABLE OF CONTENTS

LIST OF FIGURES

LIST OF TABLES

ACKNOWLEDGEMENTS

The author wishes to extend his gratitude to Dr. Gerald A. Takacs for his generous assistance and guidance in the preparation of this work. Thank you Jerry. Also a special thanks to the authors dear friend Joanne for generously devoting her time for proof reading and moral support.

I INTRODUCTION

The main purpose of this research was to obtain and investigate the photoabsorption crosssections of chlorodifluoronitrosomethane, dichlorofluoronitrosomethane and their two corresponding nitro analogs, chlorodifluoronitromethane and dichlorofluoronitromethane. The atmospheric stability of such molecules may be of environmental interest because their formation as trace amounts in the stratosphere may prevent the photochemically induced release of chlorine associated with the ozone depleting chain (1-4) [1,4].

CCL3F	+	hv	--->	CC12F	+	C1	(1)
CC12F2	+	hv	--->	CC1F2	+	C1	(2)
C1	+	03	--->	C10	+	02	(3)
C10	+	0	--->	C1	+	02	(4)

The search for chain terminating steps involving the chain centers C1 and C10 has led to investigations of coupling reactions between the chlorine cycle and the NOx cycle. Some chlorine nitrogen oxides with photoabsorption spectra that have been studied include; C1NO [3], C1NO2 [3], C1ONO [4], and C1ONO2 [5,6].

The fragments CCl2F and CClF2 are readily produced in the stratosphere from the photodecomposition of chlorofluorocarbons 11 (CCl_3F) and 12 (CCl_2F_2), respectively [2]. These halogenated methyl radicals mainly react with oxygen to produce the phosgene-like compounds CClFO and CF_2O together with the release of a second chlorine atom as either Cl or ClO [2]. Photoabsorption measurements of CClFO have been made in order to estimate the release rate of the third chlorine atom from CCl_3F [8].

The following proposed chain terminating steps (5-8) may tie up some of the chlorine in the halogenated methyl radicals as chlorine and fluorine substituted methyl nitrogen oxides.

$$CClF_2 + NO + M \longrightarrow CClF_2NO + M \quad (5)$$

$$CCl_2F + NO + M \longrightarrow CCl_2FNO + M \quad (6)$$

$$CClF_2 + NO_2 + M \longrightarrow CClF_2NO_2 + M \quad (7)$$

$$CCl_2F + NO_2 + M \longrightarrow CCl_2FNO_2 + M \quad (8)$$

The reaction of NO with $CClF_2$ [9,10] and CCl_2F [10,11] has been observed in the laboratory to produce halogen-substituted nitrosomethanes by (5) and (6) above.

Reactions analogous to (7) and (8) have been observed to occur with CF3 [12,13] and CCl3 [14] radicals although (9) may compete with (8) [15].

$$CX_3 + NO_2 \longrightarrow CX_3O + NO \qquad (9)$$

Reaction (9) takes place at low pressures with CF3 [16], however it is endothermic for CCl3 radicals at stratospheric temperatures [14].

The basis of this thesis work is the estimation of the atmospheric photochemical stability of CClF2NO, CCl2FNO, CClF2NO2 and CCl2FNO2. This involves the preparation of these compounds followed by the correlation of their respective ultraviolet and visible absorption spectra with known atmosheric solar flux data. With this information, the approximate atmospheric photodissociation rate coefficients, or J values, for each compound may be calculated.

II HISTORICAL

A) Chlorodifluoronitrosomethane

$CClF_2NO$ has been prepared by the decarboxylation of nitrosyl chlorodifluoroacetate [17], the reaction of chlorodifluoromethanesulphenylchloride with nitric acid [18], the treatment of difluoronitrosoacetic acid with hydrochloric acid [19,23] and by the photolysis of ClNO [20] and $CClF_2I$ [21] in the presence of $CClF_2H$ and NO, respectively.

Although the photoabsorption spectrum of $CClF_2NO$ has not been reported prior to this work, the wavelength for maximum absorption of visible light has been given as 650 nm in liquid acetic acid, ethanol and dimethylformamide [22]. A comprehensive study of the gas phase infrared spectrum [23] and the photoelectron spectrum [24] of $CClF_2NO$ has been conducted by Ernsting and Pfab.

B) Dichlofluoronitrosomethane

CCl_2FNO has been prepared by the reaction of dichlorofluoromethanesulphenyl chloride with nitric acid [18], the treatment of dichlorofluoronitrosoacetic acid with hydrochloric acid [23] and by the photolysis of ClNO [20] and CCl_3F [11] in the presence of CCl_2FH and NO, respectively.

The photoabsorption spectrum of CFCl2NO has not been reported prior to this work, however, the wavelength of maximum absorption by visible light has been given as 630 nmin liquid ethanol [22]. Ernsting and Pfab have examined the gas phase infrared spectrum [23] and the photoelectron spectrum of CFCl2NO [24] among other perhalonitrosomethanes.

C) Chlorodifluoronitromethane and Dichlorofluoronitromethane

CClF2NO2 has been prepared by the oxidation of CClF2NO with the oxidizing agents dimanganese heptoxide, lead dioxide and chromic oxide [21]. However, low yields (<12%) were obtained due to extensive decomposition. Using the same method, low yields were also reported for the formation of CF3NO2 from the oxidation of CF3NO [21]. Subsequent work has shown that higher yields of CF3NO2 are obtainable by using hydrogen peroxide to oxidize CF3NO [13,25]. To the knowledge of this author, a suitable method for the preparation of CCl2FNO2 has not been reported prior to this work.

The ultraviolet, visible and infrared absorption spectra of CCl3NO2 and CF3NO2 have been reported by Haszeldine [9], however, it appears that the photoabsorption spectra of CCl2FNO2 or CClF2NO2 have not been reported prior to this work.

III. EXPERIMENTAL

A. Instrumentation

1. UV-Vis Spectrophotometer and Imsai 8080 Computer Interface

A Varian Cary-219 UV-Vis spectrophotometer, equipped with a nitrogen purge facility, was used to determine ultraviolet and visible absorptions. The Cary 219 was interfaced to an Imsai 8080 microcomputer for data storage and handling. Data collected by the Imsai 8080 was stored on 8" floppy disk media in double density format.

The resolution of the Cary-219 is better than 0.05 % of full-scale transmittance in the visible and ultraviolet spectral region with a wavelength accuracy of 0.2 nm or better. The Cary-219 is capable of storing a corrected baseline. This is accomplished by pre-scanning an empty gas sample cell prior to scanning samples with the same cell.

Instrument settings used to obtain the absorption data for this work are given in Table 1.

TABLE 1. UV-Vis Spectrophotometer Instrument Settings

Control	Setting
Mode	Transmittance
Gain	Auto
Spectra Bandwidth	1 nm
Chart	5 nm/cm
Time	1 nm/sec
Responce Time	1 sec
Auto Baseline	On
Wavelength Program	700-185 nm

2. Infrared Spectrophotometer

A Perkin-Elmer 621 spectrophotometer was used to measure infrared absorptions in the region from 4000 cm-1 to 600 cm-1.

The resolution of the infrared spectrophotometer at 1000 cm-1 is 0.5 cm-1 and the wavelength accuracy is 0.5 nm as given in the Perkin-Elmer manual.

The instrument settings used throughout the experiments are given in Table 2.

TABLE 2. Infrared Spectrophotometer Settings

Control	Setting
Scale	Change
Mode	Transmittance
Source	0.8 amps
Gain	5
Slit Program	1000
Attenuator	1100
Scan Time	20
Suppression	5

3. Photolysis Apparatus

A Rayonet Photochemical Reactor, equipped with 16 Rayonet Photochemical Reactor Lamps, Cat. No. RPR- 1849 Å/2537 Å, was used to conduct photolysis experiments for this work. A cylindrical shaped cell placed inside the reactor chamber was illuminated from all sides.

B. Sample Manipulation

1. Vacuum Line and Associated Apparatus

All the gas samples in this work were handled on a Pyrex vacuum line, diagramed in Figure 1. The vacuum line was equipped with a 2 stage mercury diffusion pump, separated from the manifold by a trap cooled by a liquid nitrogen bath. The trap served to protect the manifold from mercury vapors as well as to prevent the escape of any samples into the diffusion pump. All the connections between the vacuum manifold, sample handling bulbs and gas sample cells were made with viton "O" rings and standard glass taper joints. The vacuum manifold and sample handling bulbs were fitted with greaseless Teflon stopcocks at all the connections. The vacuum manifold was also equipped with a Bendix GTC-360 thermocouple gauge for leak detection and two MKS Baratron gauges to determine pressures in the range of 10 to 1000 torr and 0.001 to 10 torr.

FIGURE 1. Vacuum Line

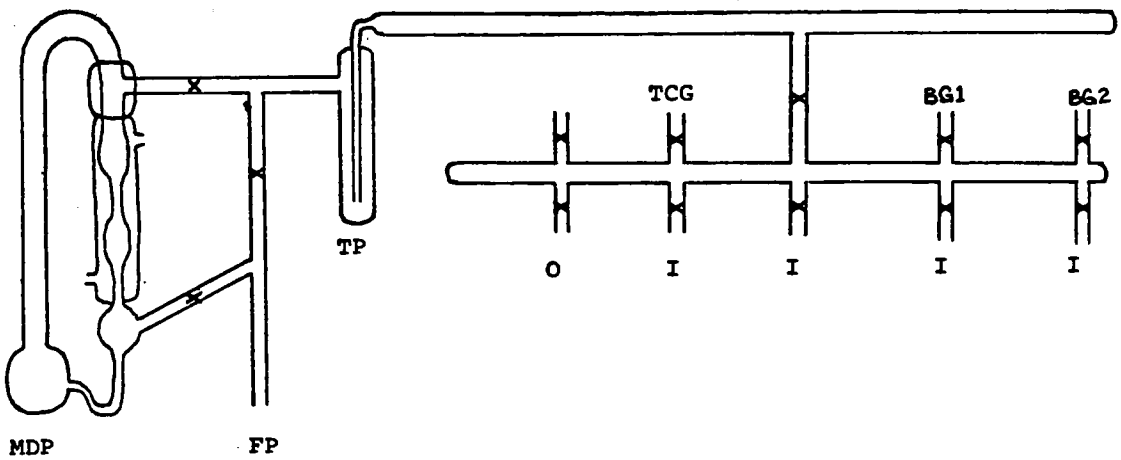

X	Stopcock
FP	Mechanical fore pump
TCG	Thermocouple gauge sensor
O	Outer standard taper joint
I	Inner standard taper joint
TP	Trap
BG1	Baratron gauge sensor (10-1000 torr)
BG2	Baratron gauge sensor (.001-10 torr)
MDP	Mercury diffusion pump

2. Sample Cells

Infrared and ultraviolet gas sample cells were made from 15/16 o.d. by 10 cm Pyrex tubing, onto which greaseless Teflon stopcocks and standard glass taper joints were glass-blown as diagramed in Figure 2. The UV cell was equipped with quartz Suprasil windows and the IR cell with potassium bromide windows. The error in the 9.99 cm pathlength for both cells was ±0.01 cm.

Also shown in Figure 2. is a sample bulb made from Vycor which has transmittance qualities in the ultraviolet that were desirable for the photolysis experiment described in section III.C.3.

A special 9 cm pathlength cell, built into a stainless steel housing, was used in low temperature studies of gas samples. The housing was designed with an inner and outer set of quartz windows separated by a sealed cavity which was purged with nitrogen or dry air to prevent the cell windows from fogging. The region containing the coolant (usually a mixture of dry-ice and acetone) did not make direct contact with the sample cell but rather with a fluid reservoir that surrounded the outer wall of the sample cell.

This reservoir consisted of a medium with a freezing point below the temperature of the coolant (usually methanol) [52].

FIGURE 2. Sample Cells

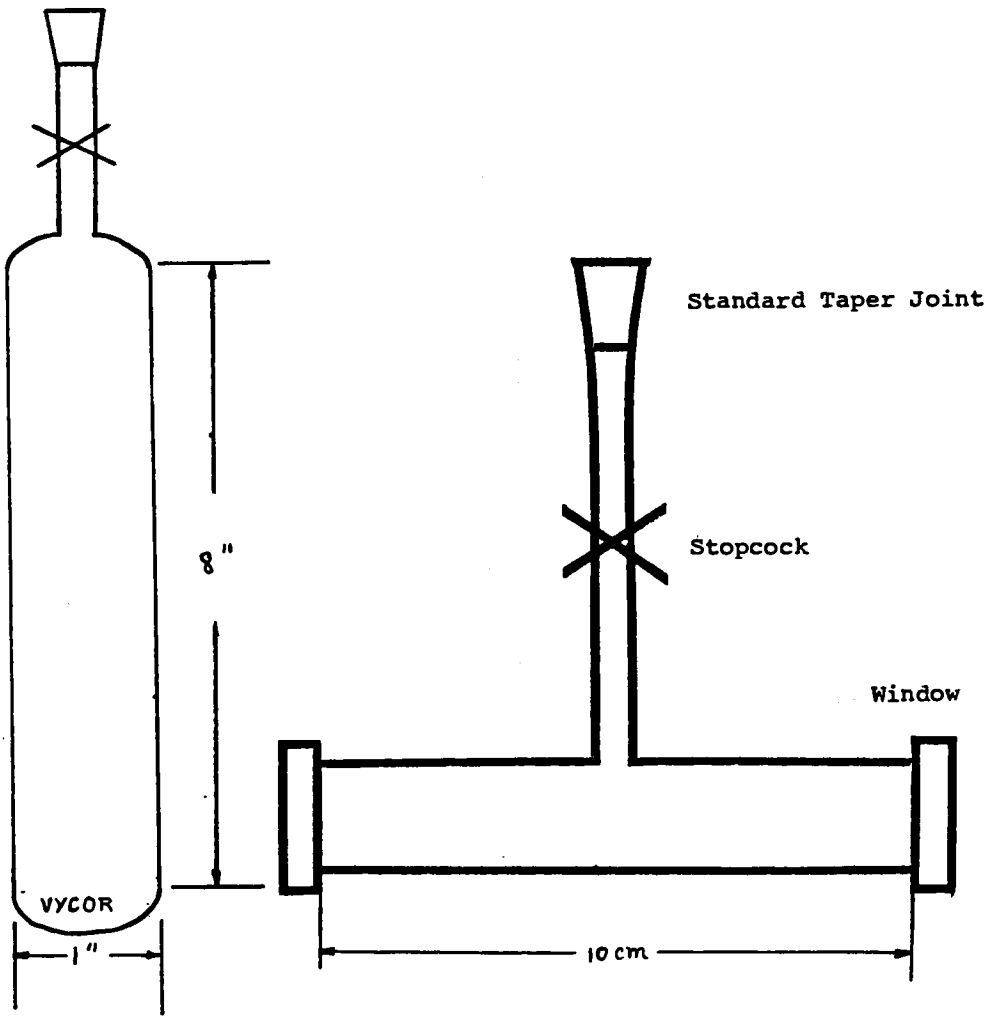

C. Synthesis of Chlorodifluoro-nitrosomethane

1) Preparation by Liquid Phase Decarboxylation

CClF2NO was prepared by bubbling nitrosyl chloride gas (Matheson >97% purity) through a well stirred slurry of sodium chlorodifluoroacetate (Pflatz and Bauer) in diglyme at 148 degrees Celsius [17].

$$CClF_2CO_2Na + ClNO \longrightarrow NaCl + CO_2 + CClF_2NO \qquad (10)$$

A steady stream of nitrogen gas directed through the reaction vessel facilitated the collection of the volatile reaction products. The resultant gases were trapped at -196 degrees Celsius (a liquid nitrogen bath) and the frozen product was outgassed by repeated pumping on the sample after thawing and recondensing the product several times. The product was purified using bulb-to-bulb distillations at the temperature of a dry-ice and acetone slush bath (-86 degrees Celsius) on a greaseless vacuum line.

In this process the frozen products are allowed to warm up to the temperature of the dry- ice and acetone slush bath and the more volatile product condenses over into a connecting flask held at the temperature of a liquid nitrogen bath (-196 degrees Celsius). The remaining distillate was discarded.

2) Preparation by Photolysis

CClF2NO was prepared by photolyzing CClF2Br in the presence of NO using radiation at a wavelength of 253.7 nm. CClF2Br (PCR Research Chemicals, Inc.) was outgassed at -196 degrees Celsius on a greaseless vacuum line using the method outlined in part 1, above. The CClF2NO product was distilled at -86 degrees Celsius (the temperature of dry-ice and acetone bath) and the middle fraction was saved and used. The vapor pressure [26] and the infrared spectrum [27] of the purified CClF2NO were consistent with the data found in the literature.

NO (Matheson >98%) was outgassed at -196 degrees Celsius and condensed into a 250 ml bulb containing approximately 10 grams of dryed granular silica-gel which assisted in the removal of NO2 impurity [32].

The frozen concentrate was distilled at the temperature of a dry-ice acetone slush bath (-86 degrees Celsius) and the pure NO collected in a connecting flask held at -196 degrees Celsius (liquid nitrogen bath).

The initial photolysis experiments were conducted in a 10 cm pathlength cell equipped with quartz-suprasil windows. Equal amounts of NO and CClF2Br were introduced into the cell on a greaseless vacuum line giving a final total pressure of approximately 1/4 atmosphere in the cell. The cell was placed inside the photolyses apparatus and illuminated with 253.7 nm radiation for approximately one day. Ultraviolet, visible and infrared scans confirmed the formation of the CF2ClNO product. BrNO and NO impurities were easily separated from the product using bulb-to-bulb distillations as outlined in part 1 above, with the utilization of a methanol slush bath at -98 degrees Celsius.

A special, large volume, reaction vessel was constructed out of Vycor glass (70% transmission at 253.7 nm, Figure 2 section III.B.2.) to improve the yield of CClF2NO. Vycor has poor transmission for radiation at 184.9 nm, present in the low pressure Hg lamps, which may result in the breakage of of C-Cl bonds in the product.

3) Preparation by Vapor Phase Decarboxylation

$CClF_2NO$ was prepared by reacting the sodium salt of chlorodifluoroacetic acid with nitrosyl chloride using a method similar to the liquid phase decarboxylation described in section III.C.1, however, with the elimination of the diglyme and the liquid phase altogether. Ten grams of finely crushed sodium chlorodifluoroacetate (Pflatz and Bauer) was placed into a 500 ml bulb equipped with a teflon greaseless stopcock, standard glass taper joint and Viton "O" ring vacuum line attachment. The bulb was evacuated on a greaseless vacuum line and the salt outgassed for at least one hour. Approximately 0.5 atmosphere of ClNO (Matheson >97% purity), previously outgassed at -196 degrees Celsius, was introduced into the bulb containing the salt. The sealed reaction bulb was removed from the vacuum line and immersed into a thermostat controlled oil bath at 145 degrees Celsius for a period of 2 to 3 days. The bulb was reattached to the vacuum line and the product outgassed using a liquid nitrogen bath (-196 degrees Celsius) and pumping on the frozen gasses for at least one hour.

Bulb- to- bulb distillations of the product using the method described in part 1, above, at the temperature of a dry- ice acetone slush bath (-86 degrees Celsius) served to remove the bulk of the more volatile CO2 and NO gas impurities. Then a very slow distillation at the temperature of a methanol slush bath (-98 degrees Celsius) separated the more volatile CClF2NO from the bulk of the unreacted ClNO. The freshly condensed blue product was warmed and allowed to expand out of its containment bulb, through a connecting column of LiOH, and condense into a bulb held at the temperature of a liquid nitrogen bath (-196 degrees Celsius). The final pure product was obtained by redistilling the product obtained in the last step at the temperature of a dry-ice acetone slush bath (-86 degrees Celsius) and collecting and saving the middle fraction.

D. Synthesis of Dichlorofluoro-nitrosomethane

CCl2FNO was prepared by reacting 16 grams of CCl2FSCl (dichlorofluorosulphenyl-chloride) with 85 ml of 33% nitric acid [18] (reaction (11)).

The reaction mixture was continuously and rigorously stirred for 4 hours while maintaining the temperature constant below 25 degrees Celsius . A steady stream of nitrogen gas, introduced into the reaction vessel, carried the freshly formed volatiles through a water trap and a phosphorous pentoxide drying tube. The product was collected in a trap cooled by a dry-ice and acetone slushbath at -86 degrees Celsius (see Figure 3.).

$$CCl2FSCl \longrightarrow CCl2FNO + CCl2FSO2Cl + NOCl + HNO3 \quad (11)$$ *

The crude product was purified on the vacuum line using bulb-to-bulb distillations, as described in section III.C.1, at the temperature of a dry-ice and acetone slush bath (-86 degrees Celsius). The middle fraction was saved and used.

The CCl2FSCl used in the preparation of CCl2FNO was made by reacting 90 grams of CCl3SCl (Kodak >98% purity) with 100 grams of HgF2 (Ozark Mahoning). The final product was distilled off from the collected fraction at 97-98 degrees Celsius [51].

* The equation for this reaction is left unbalanced due to the theoretical nature of the reaction mechanism involved [18].

FIGURE 3. Apparatus Used in the Synthesis of CCl2FNO

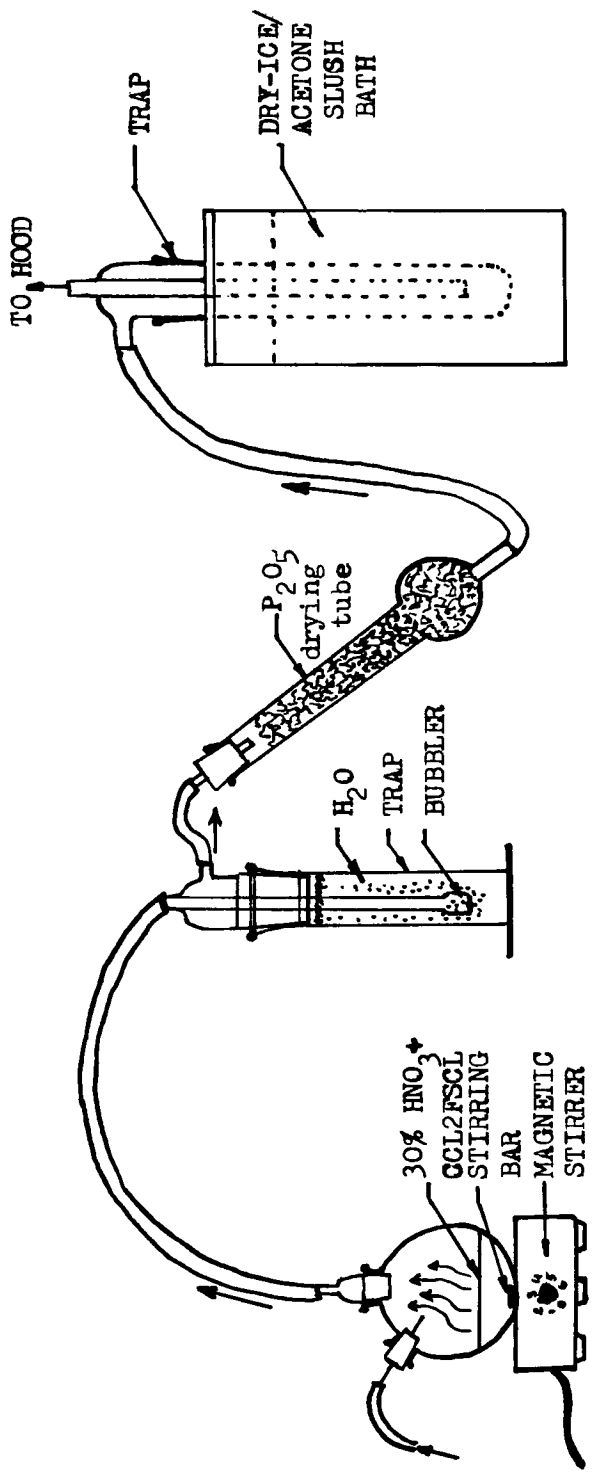

APPARATUS USED IN THE SYNTHESIS OF CCL_2FNO

E. Synthesis of Chlorodifluoronitromethane and Dichlolrofluoronitromethane

$CClF_2NO_2$ and CCl_2FNO_2 were both prepared by oxidizing their corresponding nitroso analogs with hydrogen peroxide. Approximately 400 torr of $CClF_2NO$ and CCl_2FNO were transferred individually into separate pyrex bulbs using a greaseless vacuum line. Each bulb contained 5 ml of 30% H_2O_2 that had been outgassed at -196 degrees Celsius. The same outgassing procedure outlined in section III.C.1 was followed. Each bulb was equipped with a greaseless teflon stopcock. The bulb containing the $CClF_2NO$ and H_2O_2 mixture was immersed in a thermostat controlled water bath at 50 degrees Celsius for a period of 3 to 4 days. During this time the bulb containing the CCl_2FNO was left at room temperature (approximately 25 degrees Celsius). After 12 hours, the bulb containing the CCl_2FNO and H_2O_2 mixture was connected to the vacuum line and the faint blue gas phase was transferred into another bulb containing a fresh supply of 5 ml of 30% H_2O_2. The mixture was allowed to react at room temperature for an additional 2 to 3 days. Under these conditions both of the initially blue gas samples were nearly colorless by the fourth day.

The remaining steps involve distillation of the contents in each of the reaction bulbs to separate the nitro compounds from their respective nitroso compounds and other volatile impurities formed during the oxidation process. The vapor phase containing the CClF2NO2 product was separated from the residual liquids in its reaction bulb by distillation at the temperature of a chloroform slush bath (-63 degrees Celsius). The volatile fraction containing the bulk of the CClF2NO was redistilled at the temperature of a methanol slush bath (-98 degrees Celsius). The more volatile blue fraction containing the bulk of the unreacted CClF2NO was discarded and the less volatile colorless CClF2NO2 was saved and used. The vapor phase containing the CCl2FNO2 was isolated from the less volatile liquids remaining in the reaction bulb by distilling the liquid at the temperature of a carbon-tetrachloride slush bath (-22 degrees Celsius) and collecting the volatile fraction at the temperature of a liquid nitrogen bath (-196 degrees Celsius). The more volatile blue colored fraction was redistilled at the temperature of a dry-ice acetone slush bath.

This separated the more volatile fraction containing any unreacted CCl2FNO from the remaining fraction containing the CCl2FNO2 product. The CCl2FNO2 product was further purified by passing the gas through a short column of dried granular CaCl2 to remove the NO2 impurity that was detected in the UV-Vis spectrum of the compound (see section IV.B.1).

The colorless CClF2NO2 and CCl2FNO2 were stored in the dark at the temperature of a dry-ice and acetone slush bath (-86 degrees Celsius). This precaution was taken to prevent the occurance of photo or thermal decomposition although none had been observed during the course of experiments.

IV. RESULTS AND DISCUSSION

A. Chlorodifluoronitrosomethane and Dichlorfluoronitrosomethane

1. Preparation and Purity

In the preparation of CClF2NO, reaction (10) procedes with the formation of NaCl and the stable nitrosylchlorodifluoroacetate, CClF2COONO, which is susequently pyrolyzed [29].

$$CF_2ClCO_2Na + ClNO \xrightarrow{148\ C} NaCl + CO_2 + CClF_2NO \qquad (10)$$

$CClF_2NO$ is formed with the liberation of CO_2 during the pyrolysis of the nitrosylchlorodifluoroacetate.

As can be observed in the infrared spectra of samples taken between bulb-to-bulb distillations for the purpose of establishing the purity of $CClF_2NO$, it was often impossible to adequately separate the $CClF_2NO$ product from large quantities of unreacted ClNO when employing the synthesis described previously in section III.C.1. A modification of this synthesis, described in section III.C.3., was successfully utilized in obtaining the pure $CClF_2NO$ used in this work. In this procedure the diglyme, which had constituted the liquid phase of the reaction, was eliminated to allow a solid surface-to-gas phase reaction to occur between the salt and NOCl. The modified reaction was conducted at the same temperature as the liquid phase reaction.

Reaction (7) had previously been utillized by Tattershall [20] in the preparation of $CClF_2NO$ from the gas phase photolysis of ClNO in a mixture of $CClF_2H$ and NO.

$$CClF_2 + NO_2 + M \longrightarrow CClF_2NO_2 + M \quad (7)$$

$$ClNO + h\nu \longrightarrow Cl + NO$$

$$Cl + CClF_2H \longrightarrow HCl + CClF_2$$

$$CClF_2 + NO + M \longrightarrow CClF_2NO + M \qquad (5)$$

However, the $CClF_2NO$ was difficult to separate from ClNO used in the reaction [20]. To avoid this separation difficulty completely and at the same time utillize an alternate method of preparing $CClF_2NO$, CF_2ClBr was photolyzed in the presence of NO as described in section III.C.2. Photodissociation of $CClF_2Br$ occurs predominantly by the breakage of the weakest bond, which in this case is the C-Br bond [30]. Separation of BrNO, instead of ClNO, from $CClF_2NO$ using bulb-to-bulb distillations is easily achieved due to the larger difference in vapor pressures between $CClF_2NO$ and BrNO as compared to the more volatile ClNO. Preparation of $CClF_2NO$ by the photolyses of $CClF_2BR$ resulted in less product yield as compared to the decarboxylation method described in section III.C.3 although the IR and UV-Vis spectra of the purified $CClF_2NO$ product obtained from both reactions were consistant with each other.

CCl2FNO was prepared using the method described in section III.D. The difficulty with separating the ClNO impurity from the final product was not encountered as in the preparation of CClF2NO due to a greater difference in vapor pressures however NO2 impurity as observed by UV-vis spectroscopy proved to be very difficult to remove without redistilling the product and ending up with less product. The overall yield of CCl2FNO by this reaction exceeded the amounts of CClF2NO obtained using the decarboxylation reaction. The product was approximately equal in volume (liquid form) to the amount of the parent compound, CCl2FSCL, that had been used in the reaction.

Because CCl2FNO and CClF2NO are both gases at room temperature, the yields can most conveniently be judged by the final pressures used in measuring the UV-Vis spectra of the compounds, assuming the same cell is used for both compounds. These pressures need not exceed one atmosphere due to the high extinction coefficients which are characteristic of these compounds.

The purified CClF2NO and CCl2FNO were deep blue in color and were stored in the dark to prevent photodecomposition. The infrared spectra of the compounds were in agreement with the spectra reported by Ernsting and Pfab [24] (see Figures 4 and 5 for the IR spectra of CClF2NO and CCl2FNO).

Vapor pressure measurements for CClF2NO and CCl2FNO were made over a range of temperatures and are given in Table 3. The following linear expressions were obtained from the data using the method of least-squares:

$$\ln P\ (\text{torr}) = -2620 / T\ (\text{K}) + 17.62$$

$$\ln P\ (\text{torr}) = -2923 / T\ (\text{K}) + 16.75$$

for CClF2NO and CCl2FNO respectively. A plot of this data is shown in Fig 6. Extrapolation of the vapor pressure curves to 760 torr gave -34.5 and 16 degrees Celsius for the boiling points of CClF2NO and CCl2FNO, respectively. These boiling points are within one percent of the previously reported values of -35 and 15 degrees Celsius [9]. Using the Clausius-Clapeyron equation, the heats of vaporization of CClF2NO and CCl2FNO were calculated to be 5.2 and 5.8 Kcal/mol, respectively.IV.A.2.

FIGURE 4 The Infrared Spectrum of CClF2NO at 298 K. Pressure = 20 torr, Pathlength = 10 cm.

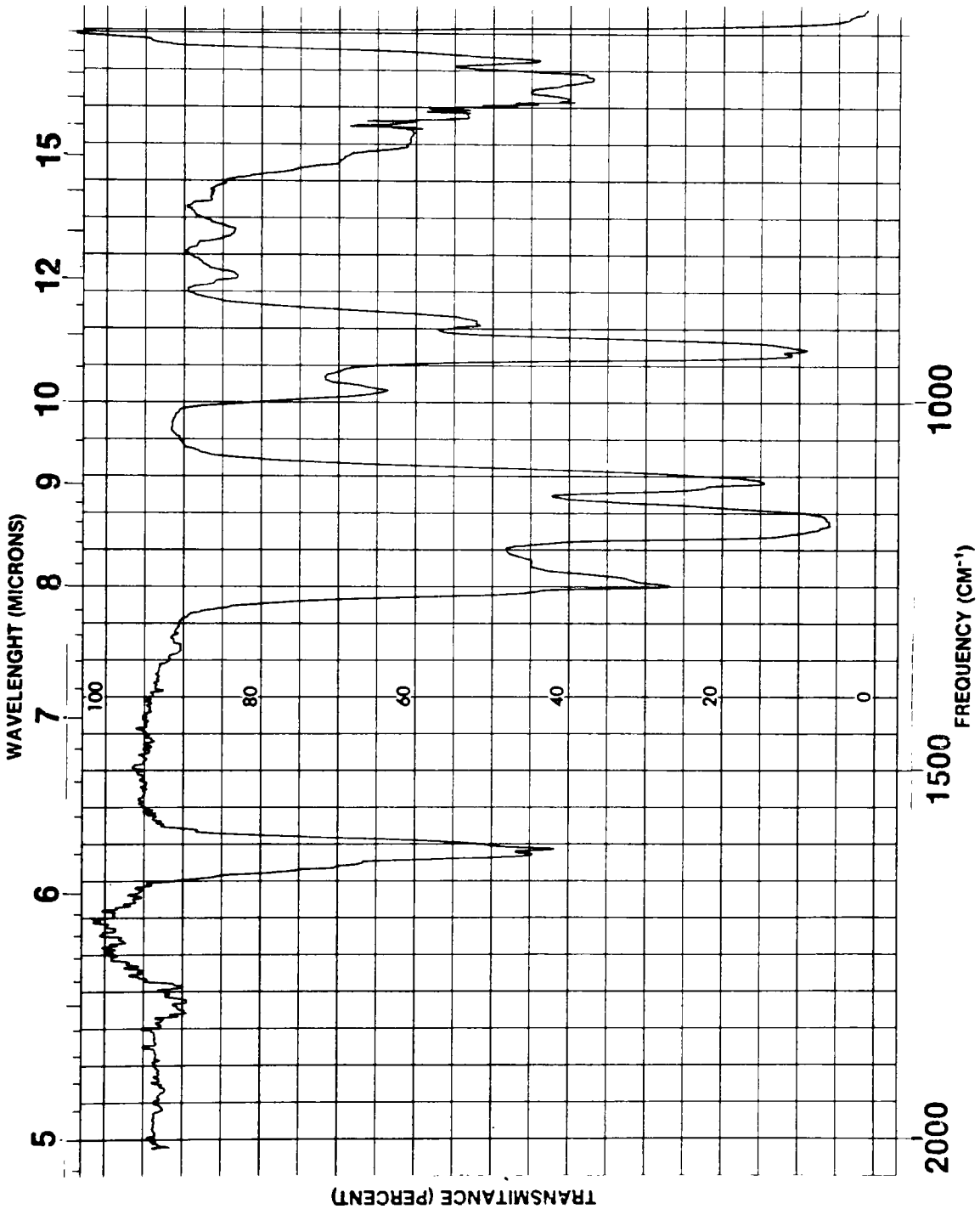

FIGURE 5. The Infrared Spectrum of CCl2FNO at 298 K. Pressure = 10 torr, Pathlength = 10 cm.

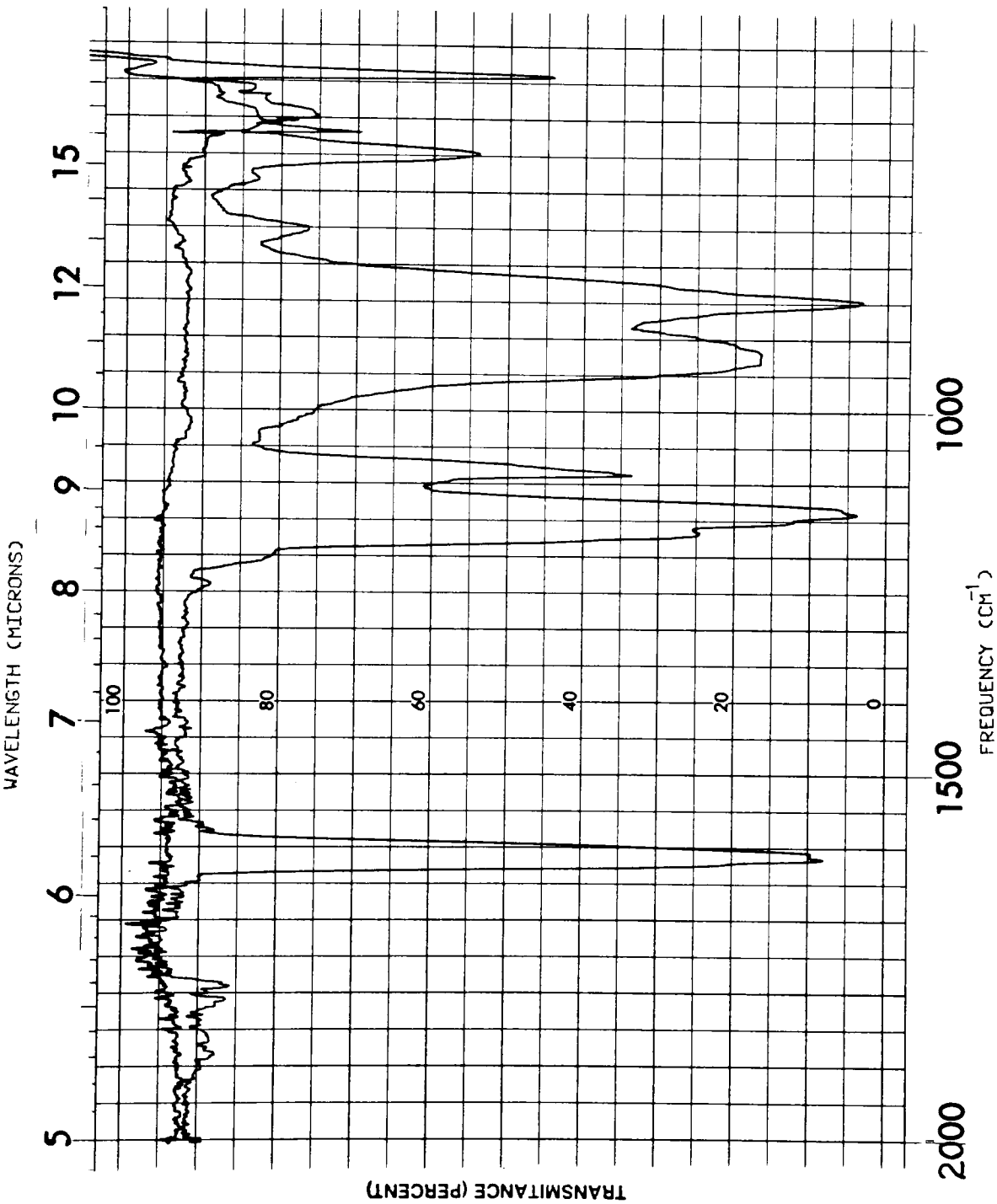

TABLE 3

Vapor Pressure Data for CClF2NO, CCl2FNO, CClF2NO2 and CCl2FNO2

	ln P (Torr)			
Temp.(C)	CClF2NO	CCl2FNO	CClF2NO2	CCl2FNO2
-131.4	0.53			
-122.8	0.92			
-110.8	1.44			
- 97.8	2.67	1.64		
- 86.0	3.60	1.44	1.22	-2.12
- 63.5	5.11	2.73	2.38	-0.16
- 45.2		3.81	3.38	1.01
- 22.9		5.08	4.76	2.73
0			5.70	4.01

FIGURE 6. Temperature Dependence of the Vapor Pressure of CClF2NO and CCl2FNO

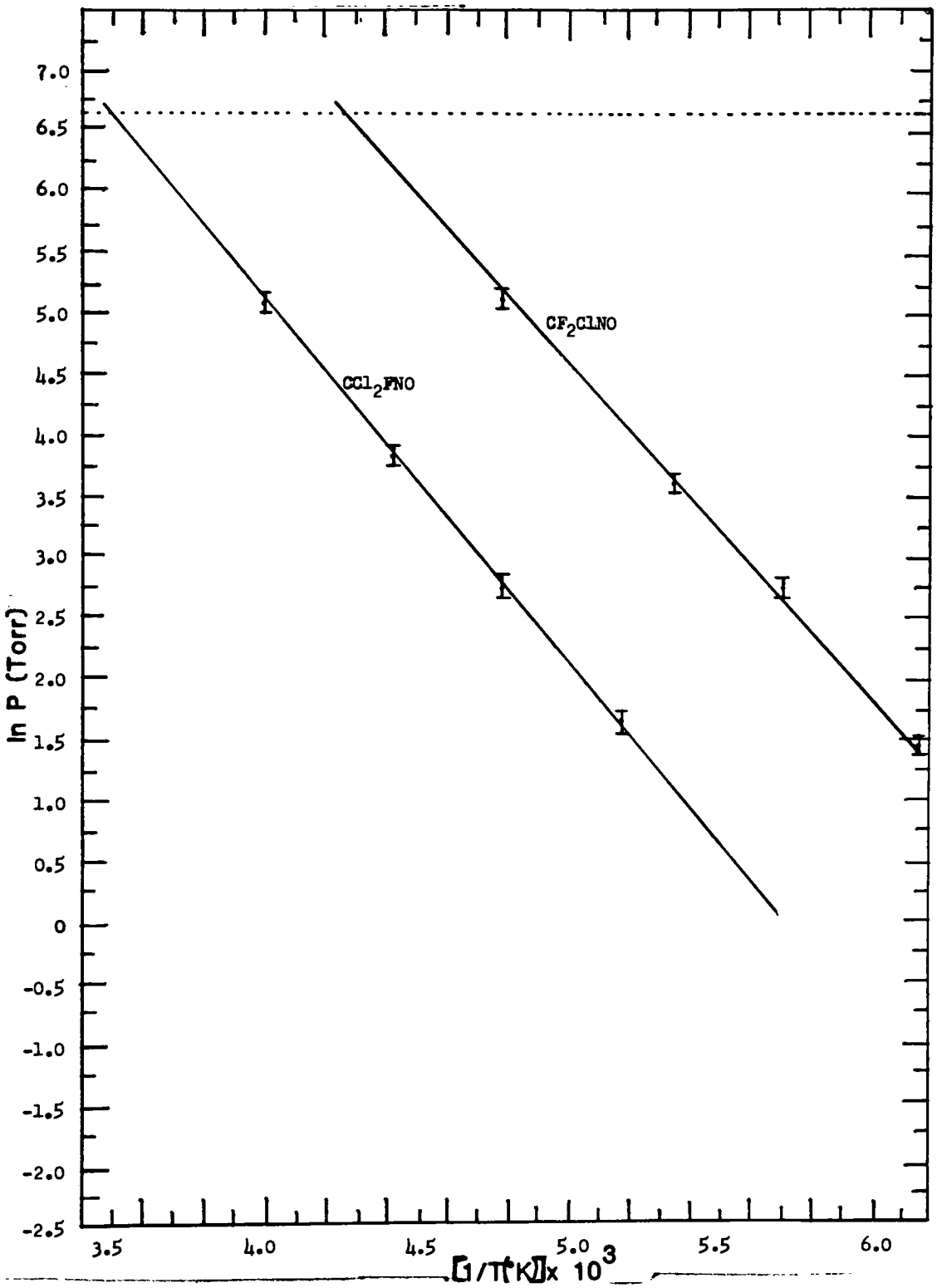

2 The Absorption Cross-Sections of CClF2NO and CCl2FNO

Shown in Figures 7 and 8 are the photoabsorption spectra of CClF2NO and CCl2FNO, which are computer averages of spectra taken over a range of sample pressures from 0.5 to 215 torr and 0.3 to 400 torr, respectively, for each compound. The average cross-sections at each wavelength are given in Tables 4 and 5.

The fine structure which is apparent in the visible absorption region of both compounds (see Figures 9 and 10) is also observed for CH3NO [37-39], CD3NO [39], CCl3NO [1], and CF3NO [1,40]. The corresponding wavelengths for the peaks in the visible fine structure region are given for CClF2NO and CCl2FNO in Tables 6 and 7, respectively. The data defining the fine structure region was taken utilizing a constant spectral bandwidth of one nm on the Cary-219 UV-Vis spectrophotometer. The gaseous compounds were cooled using the special sample cell described in section III.B.2 in order to quench thermal energy and obtain the spectral resolution shown in Figures 9 and 10.

The appearance of these bands can be attributed to the excited vibrational modes of the n -- π^* transition involving nitrogen non-bonding electrons. The absorption maxima occur at 642.5 and 633 nm at room temperature for gaseous CClF2NO and CCl2FNO, respectively and are in close agreement with the reported values of 650 nm for CClF2NO in liquid acetic acid, ethanol and dimethyl formamide and 630 nm for CCl2FNO in liquid ethanol [22].

FIGURE 7. UV-Vis Absorption Spectrum of Gaseous CClF2NO at 298 K.

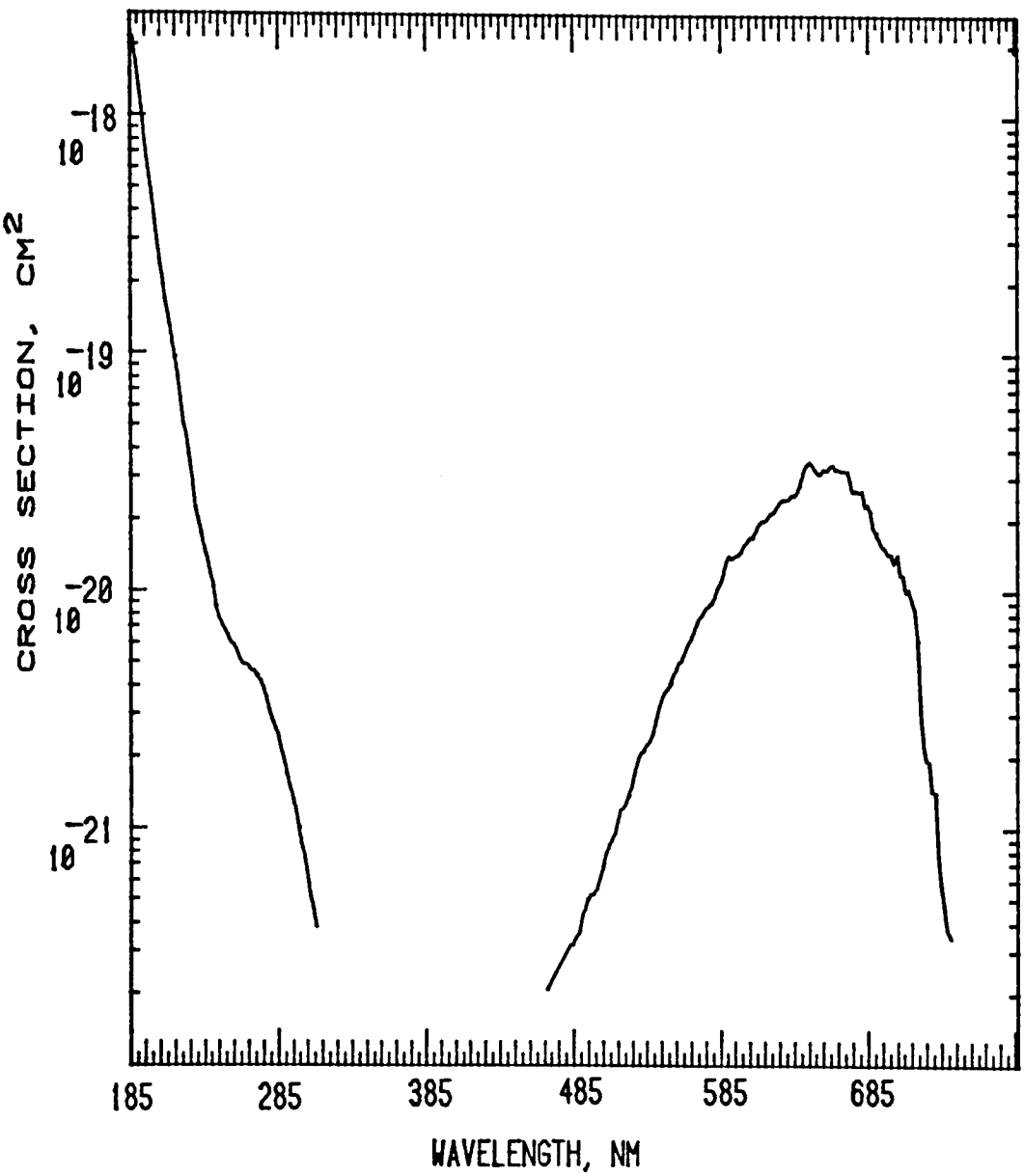

FIGURE 8. UV-Vis Absorption Spectrum of Gaseous CCl2FNO at 298 K.

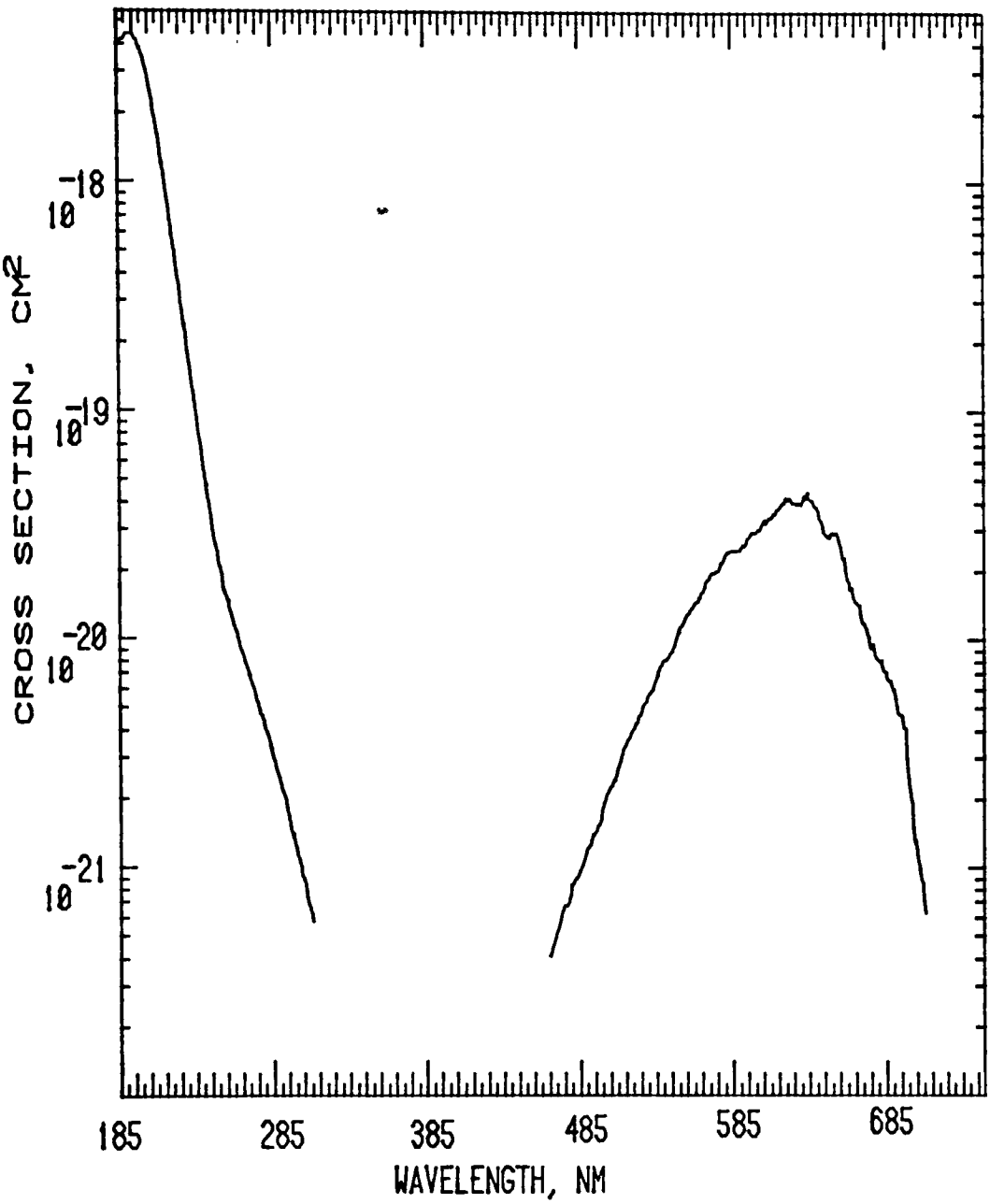

TABLE 4. Averaged Cross-Section Data for CClF2NO Wavelength (nm), Cross-Section (σ)

λ	σ
185	2.18776E-18
187	1.69824E-18
189	1.31825E-18
191	1.04713E-18
193	7.94328E-19
195	6.16595E-19
197	4.89779E-19
199	3.89046E-19
201	3.09030E-19
203	2.45470E-19
205	2.08929E-19
207	1.69824E-19
209	1.44544E-19
211	1.17490E-19
213	9.77237E-20
215	8.31765E-20
217	6.45653E-20
219	5.24805E-20
221	4.36515E-20
223	3.54813E-20
225	2.95120E-20
227	2.23873E-20
229	1.99526E-20
231	1.77828E-20
233	1.51356E-20
235	1.34896E-20
237	1.17490E-20
239	1.07152E-20
241	8.70964E-21
243	7.76246E-21
245	7.24438E-21
247	6.76082E-21
249	6.45651E-21
251	6.02560E-21
253	5.88844E-21
255	5.62340E-21
257	5.24807E-21
259	5.01185E-21
261	5.01185E-21
263	4.89779E-21
265	4.67735E-21
267	4.57087E-21
269	4.38515E-21
271	4.16867E-21
273	3.89045E-21
275	3.54812E-21
277	3.16228E-21
279	2.95120E-21
281	2.75424E-21
283	2.51189E-21
285	2.18777E-21
287	1.94985E-21
289	1.73780E-21
291	1.54882E-21
293	1.34896E-21
295	1.17490E-21
297	1.00000E-21
299	8.51138E-22
301	7.58575E-22
303	6.45853E-22
305	5.37030E-22
307	4.46682E-22
309	3.80190E-22
311	2.81839E-22
313	2.34422E-22
315	1.90546E-22
317	1.65958E-22
319	1.34896E-22
321	1.41254E-22
323	1.17489E-22
325	1.09648E-22
327	9.12008E-23
329	7.94327E-23
331	7.58574E-23
333	7.41310E-23
335	7.41310E-23
337	7.41310E-23
339	7.76243E-23
341	7.94327E-23
343	8.31762E-23
345	8.12008E-23
347	1.04713E-22
349	1.09648E-22
351	1.17489E-22
353	1.20226E-22
355	1.25893E-22
357	1.31825E-22
359	1.38038E-22
361	1.44544E-22
363	1.47911E-22
365	1.69824E-22
367	1.62181E-22
369	1.69824E-22
371	1.69824E-22
373	1.77828E-22
375	1.77828E-22
377	1.81970E-22
379	1.81970E-22
381	1.90546E-22
383	1.99526E-22
385	2.08929E-22
387	2.04173E-22
389	2.08929E-22
391	2.08929E-22
393	1.94984E-22
395	2.04173E-22
397	1.94984E-22
399	1.99526E-22
401	2.08929E-22
403	1.99526E-22
405	2.13797E-22
407	2.18776E-22
409	2.29087E-22
411	2.18776E-22
413	2.23872E-22
415	2.08929E-22
417	2.08929E-22
419	2.18776E-22
421	2.13797E-22
423	2.18778E-22
425	2.04173E-22
427	2.04173E-22
429	1.86208E-22
431	2.08929E-22
433	1.94984E-22
435	2.23872E-22
437	1.77828E-22
439	2.29087E-22
441	1.73780E-22
443	1.77828E-22
445	2.08929E-22
447	1.94964E-22
449	1.94984E-22
451	1.86208E-22
453	1.94964E-22
455	1.94984E-22
457	2.04173E-22
459	1.94984E-22
461	2.08929E-22
463	2.39883E-22
465	2.08929E-22
467	2.23872E-22
469	2.08929E-22
471	2.18776E-22
473	2.51169E-22
475	2.75423E-22
477	2.63028E-22
478	3.01995E-22
481	3.23594E-22
483	3.23594E-22
485	3.46736E-22
487	3.63077E-22
489	4.26578E-22

λ	σ
491	4.57088E-22
493	5.12860E-22
495	5.37030E-22
497	5.37030E-22
499	5.62339E-22
501	6.16592E-22
503	6.91829E-22
505	7.76244E-22
507	8.31763E-22
509	9.12010E-22
511	9.77235E-22
513	1.07152E-21
515	1.20226E-21
517	1.25893E-21
519	1.31825E-21
521	1.41254E-21
523	1.58489E-21
525	1.77828E-21
527	1.94985E-21
529	2.08929E-21
531	2.18777E-21
533	2.29087E-21
535	2.39884E-21
537	2.57040E-21
539	2.88403E-21
541	3.16228E-21
543	3.46736E-21
545	3.71535E-21
547	3.89045E-21
549	4.07380E-21
551	4.46682E-21
553	4.78630E-21
555	5.12859E-21
557	5.24807E-21
559	5.62340E-21
561	6.02560E-21
563	6.30955E-21
565	6.76082E-21
567	7.24438E-21
569	7.76246E-21
571	8.31765E-21
573	8.70964E-21
575	8.91248E-21
577	9.12011E-21
579	9.54992E-21
581	1.02329E-20
583	1.09647E-20
585	1.20228E-20
587	1.34896E-20
589	1.41254E-20
591	1.38038E-20
593	1.41254E-20
595	1.44544E-20
597	1.51356E-20
599	1.62181E-20

λ	σ
601	1.65959E-20
603	1.73780E-20
605	1.73780E-20
607	1.81971E-20
609	1.94984E-20
611	1.99526E-20
613	1.99526E-20
615	2.04174E-20
617	2.13796E-20
619	2.18777E-20
621	2.29087E-20
623	2.39883E-20
625	2.45471E-20
627	2.45471E-20
629	2.45471E-20
631	2.57040E-20
633	2.63027E-20
635	2.69155E-20
637	2.88402E-20
639	3.16228E-20
641	3.38845E-20
643	3.54813E-20
645	3.46736E-20
647	3.31131E-20
649	3.16228E-20
651	3.16228E-20
653	3.31131E-20
655	3.23593E-20
657	3.38845E-20
659	3.46736E-20
661	3.31131E-20
663	3.31131E-20
665	3.23593E-20
667	3.23593E-20
669	3.23593E-20
671	3.01994E-20
673	2.69155E-20
675	2.75423E-20
677	2.69155E-20
679	2.75423E-20
681	2.29087E-20
683	2.34423E-20
685	2.18777E-20
687	1.86209E-20
689	1.77828E-20
691	1.69824E-20
693	1.58489E-20
695	1.54882E-20
697	1.44544E-20
699	1.44544E-20
701	1.31825E-20
703	1.44544E-20
705	1.17490E-20
707	1.17490E-20

λ	σ
709	9.99998E-21
711	1.02329E-20
713	9.54992E-21
715	8.51139E-21
717	6.16593E-21
719	3.16228E-21
721	2.29087E-21
723	1.94985E-21
725	1.90547E-21
727	1.47911E-21
729	1.44544E-21
731	7.76244E-22
733	5.75440E-22
735	4.78630E-22
737	3.80190E-22
739	3.46736E-22
741	2.81839E-22
743	2.75423E-22
745	2.39883E-22
747	2.18776E-22
749	2.04173E-22
751	2.18776E-22
753	1.77828E-22
755	1.44544E-22
757	1.02329E-22
759	9.12008E-23
761	8.70964E-23
763	7.07946E-23
765	6.30956E-23
767	6.30956E-23
769	5.37030E-23
771	3.89045E-23
773	3.31132E-23
775	2.13796E-23
777	2.29086E-23
779	1.99526E-23
781	1.99526E-23
783	1.86209E-23
785	1.44544E-23
787	9.99999E-23
789	1.07152E-21
791	1.14815E-21
793	1.20226E-21

TABLE 5. Averaged Cross-Section Data for CCl2FNO Wavelength (nm), Cross-Section (σ)

λ	σ
185	3.96712E-18
186	4.04259E-18
187	4.14989E-18
188	4.20382E-18
189	4.30368E-18
190	4.40587E-18
191	4.45153E-18
192	4.45752E-18
193	4.45487E-18
194	4.43998E-18
195	4.38483E-18
196	4.2577E-18
197	4.12717E-18
198	4.00061E-18
199	3.83854E-18
200	3.65057E-18
201	3.48274E-18
202	3.2775E-18
203	3.0731E-18
204	2.87654E-18
205	2.6677E-18
206	2.46682E-18
207	2.27371E-18
208	2.00735E-18
209	1.83501E-18
210	1.67363E-18
211	1.51823E-18
212	1.37308E-18
213	1.24021E-18
214	1.10816E-18
215	9.93694E-19
216	8.86753E-19
217	7.92274E-19
218	7.06164E-19
219	6.29266E-19
220	5.47417E-19
221	4.95957E-19
222	4.40209E-19
223	3.9033E-19
224	3.46098E-19
225	3.07181E-19
226	2.73198E-19
227	2.40632E-19
228	2.1565E-19
229	1.91206E-19
230	1.7036E-19
231	1.51328E-19
232	1.34292E-19
233	1.1965E-19
234	1.0613E-19
235	9.42467E-20
236	8.37999E-20
237	7.4743E-20
238	6.66574E-20
239	5.95115E-20
240	5.32059E-20
241	4.76956E-20
242	4.28112E-20
243	3.85271E-20
244	3.47777E-20
245	3.15082E-20
246	2.86084E-20
247	2.61038E-20
248	2.39107E-20
249	2.20443E-20
250	2.03846E-20
251	1.89293E-20
252	1.74816E-20
253	1.63333E-20
254	1.5316E-20
255	1.44135E-20
256	1.36028E-20
257	1.28664E-20
258	1.20814E-20
259	1.14455E-20
260	1.08838E-20
261	1.03746E-20
262	9.86699E-21
263	9.32029E-21
264	8.86889E-21
265	8.43697E-21
266	8.0308E-21
267	7.64327E-21
268	7.21041E-21
269	6.85737E-21
270	6.52207E-21
271	6.20167E-21
272	5.90215E-21
273	5.59692E-21
274	5.32256E-21
275	5.04313E-21
276	4.79396E-21
277	4.54829E-21
278	4.32249E-21
279	4.10124E-21
280	3.88784E-21
281	3.68417E-21
282	3.49508E-21
283	3.30368E-21
284	3.12475E-21
285	2.9544E-21
286	2.79622E-21
287	2.64561E-21
288	2.50796E-21
289	2.3562E-21
290	2.22654E-21
291	2.10089E-21
292	1.98157E-21
293	1.85366E-21
294	1.7428E-21
295	1.6008E-21
296	1.48162E-21
297	1.4038E-21
298	1.33309E-21
299	1.21929E-21
300	1.12786E-21
301	1.07161E-21
302	9.94188E-22
303	9.43336E-22
304	8.81225E-22
305	8.33996E-22
306	7.77183E-22
307	7.15739E-22
308	6.65795E-22
309	6.22428E-22
310	5.77581E-22
311	5.55207E-22
312	5.32866E-22
313	5.04189E-22
314	4.66032E-22
315	4.53337E-22
316	4.02654E-22
317	4.2164E-22
318	3.91589E-22
319	3.60018E-22
320	3.66327E-22
321	3.41108E-22
322	3.37958E-22
323	3.19075E-22
324	3.06499E-22
325	3.12784E-22
326	2.97072E-22
327	3.01785E-22
328	2.87652E-22
329	3.03356E-22
330	2.92361E-22
331	2.87652E-22
332	2.89222E-22
333	2.95504E-22
334	2.7824E-22
335	2.84514E-22
336	2.90795E-22
337	2.75103E-22
338	2.93933E-22
339	3.01785E-22
340	3.01785E-22
341	3.03356E-22
342	3.00214E-22
343	2.82945E-22
344	2.97072E-22
345	2.97072E-22
346	3.04927E-22
347	2.97072E-22
348	3.2222E-22
349	2.98644E-22
350	2.93933E-22
351	3.08069E-22
352	3.08069E-22
353	3.03356E-22
354	3.39533E-22
355	3.09641E-22
356	3.08069E-22
357	3.28514E-22
358	3.08069E-22
359	2.92361E-22
360	3.01785E-22
361	3.06499E-22
362	3.04927E-22
363	2.95504E-22
364	2.97072E-22
365	3.23794E-22
366	3.06499E-22
367	3.17501E-22
368	3.11213E-22
369	3.06499E-22
370	2.97072E-22
371	2.90795E-22
372	3.09641E-22
373	2.86085E-22
374	2.81375E-22
375	2.87652E-22
376	3.04927E-22
377	2.75103E-22
378	2.6883E-22
379	2.82945E-22
380	2.89222E-22
381	2.81375E-22
382	2.7824E-22
383	2.71964E-22
384	2.87652E-22
385	2.82945E-22
386	2.67263E-22
387	2.67263E-22
388	2.64128E-22
389	2.70398E-22
390	2.6883E-22
391	2.67263E-22
392	2.64128E-22
393	2.50033E-22
394	2.4377E-22
395	2.57861E-22
396	2.469E-22
397	2.39074E-22
398	2.67263E-22
399	2.42204E-22
400	2.60995E-22
401	2.51597E-22
402	2.28127E-22
403	2.26564E-22
404	2.35946E-22
405	2.45336E-22
406	2.25E-22
407	2.09378E-22
408	2.54729E-22
409	2.4064E-22
410	2.48465E-22
411	2.21873E-22
412	2.21873E-22
413	2.62563E-22
414	2.20311E-22
415	2.14062E-22
416	2.03132E-22
417	2.10939E-22
418	2.21873E-22
419	2.26564E-22
420	2.2969E-22
421	2.25E-22
422	2.28127E-22
423	2.28127E-22

λ	σ
424	2.3751E-22
425	2.15624E-22
426	1.9221E-22
427	2.23437E-22
428	2.28127E-22
429	2.01573E-22
430	2.25E-22
431	2.39074E-22
432	2.07816E-22
433	2.21873E-22
434	2.3751E-22
435	2.60995E-22
436	2.39074E-22
437	2.09378E-22
438	2.26564E-22
439	2.7824E-22
440	2.4064E-22
441	2.12499E-22
442	2.20311E-22
443	2.35946E-22
444	2.71964E-22
445	2.82945E-22
446	2.57861E-22
447	2.84514E-22
448	3.2222E-22
449	2.81375E-22
450	2.81375E-22
451	2.86085E-22
452	3.09641E-22
453	3.11213E-22
454	3.14359E-22
455	3.31662E-22
456	3.23794E-22
457	3.48986E-22
458	3.61597E-22
459	3.64751E-22
460	3.93171E-22
461	3.97911E-22
462	4.07398E-22
463	4.56509E-22
464	4.42235E-22
465	4.20059E-22
466	4.50165E-22
467	4.85099E-22
468	4.97821E-22
469	5.15335E-22
470	5.45627E-22
471	5.71186E-22
472	5.98388E-22
473	6.38476E-22
474	6.78669E-22
475	6.88332E-22
476	6.91553E-22
477	7.23812E-22
478	7.59372E-22
479	8.22614E-22
480	8.60035E-22
481	9.00811E-22
482	9.15518E-22
483	9.36786E-22
484	9.69561E-22
485	1.00241E-21
486	1.03203E-21
487	1.07161E-21
488	1.16105E-21
489	1.21096E-21
490	1.25435E-21
491	1.29116E-21
492	1.35158E-21
493	1.39874E-21
494	1.45112E-21
495	1.48501E-21
496	1.5428E-21
497	1.59567E-21
498	1.67103E-21
499	1.7896E-21
500	1.88487E-21
501	1.99168E-21
502	2.09544E-21
503	2.18972E-21
504	2.28126E-21
505	2.35131E-21
506	2.39021E-21
507	2.45961E-21
508	2.56339E-21
509	2.70136E-21
510	2.85386E-21
511	3.00751E-21
512	3.16444E-21
513	3.28607E-21
514	3.4023E-21
515	3.51208E-21
516	3.64287E-21
517	3.74728E-21
518	3.8604E-21
519	3.97093E-21
520	4.07407E-21
521	4.23026E-21
522	4.40183E-21
523	4.6244E-21
524	4.81726E-21
525	5.06588E-21
526	5.2307E-21
527	5.41459E-21
528	5.5221E-21
529	5.66799E-21
530	5.75248E-21
531	5.90388E-21
532	6.0736E-21
533	6.35273E-21
534	6.59956E-21
535	6.9341E-21
536	7.18418E-21
537	7.51239E-21
538	7.74133E-21
539	7.9872E-21
540	8.22207E-21
541	8.40733E-21
542	8.5788E-21
543	8.67471E-21
544	8.85768E-21
545	9.09711E-21
546	9.43109E-21
547	9.77925E-21
548	1.03016E-20
549	1.07405E-20
550	1.11805E-20
551	1.15419E-20
552	1.18321E-20
553	1.21023E-20
554	1.24499E-20
555	1.28421E-20
556	1.31619E-20
557	1.34324E-20
558	1.37493E-20
559	1.40009E-20
560	1.42948E-20
561	1.46819E-20
562	1.5165E-20
563	1.56534E-20
564	1.62847E-20
565	1.67831E-20
566	1.73175E-20
567	1.78999E-20
568	1.83751E-20
569	1.8798E-20
570	1.90239E-20
571	1.93539E-20
572	1.93072E-20
573	1.94177E-20
574	1.97652E-20
575	2.01608E-20
576	2.07575E-20
577	2.12022E-20
578	2.20014E-20
579	2.27329E-20
580	2.32592E-20
581	2.38723E-20
582	2.3925E-20
583	2.44393E-20
584	2.45413E-20
585	2.45722E-20
586	2.47071E-20
587	2.43471E-20
588	2.45309E-20
589	2.46666E-20
590	2.49195E-20
591	2.55999E-20
592	2.62097E-20
593	2.71331E-20
594	2.82376E-20
595	2.88213E-20
596	2.96011E-20
597	3.00055E-20
598	2.98912E-20
599	3.0165E-20
600	3.02634E-20
601	3.08317E-20
602	3.12568E-20
603	3.16299E-20
604	3.22195E-20
605	3.29292E-20
606	3.26601E-20
607	3.33484E-20
608	3.38127E-20
609	3.3916E-20
610	3.46564E-20
611	3.53141E-20
612	3.56318E-20
613	3.68669E-20
614	3.75223E-20
615	3.7668E-20
616	3.92441E-20
617	3.97255E-20
618	4.00818E-20
619	4.13903E-20
620	4.07518E-20
621	4.15955E-20
622	4.17136E-20
623	4.02172E-20
624	3.98886E-20
625	3.96643E-20
626	3.92494E-20
627	4.01315E-20
628	4.02456E-20
629	3.93025E-20
630	4.11588E-20
631	4.24602E-20
632	4.12375E-20
633	4.36335E-20
634	4.1917E-20
635	4.06103E-20
636	4.11595E-20
637	3.95203E-20
638	3.7741E-20
639	3.78978E-20
640	3.60531E-20
641	3.36101E-20
642	3.27462E-20
643	3.14102E-20
644	2.98865E-20
645	2.96263E-20
646	2.91534E-20
647	2.85963E-20
648	2.97416E-20
649	3.01612E-20
650	2.93613E-20
651	3.00032E-20
652	3.02613E-20
653	2.85937E-20
654	2.73172E-20
655	2.51156E-20
656	2.35888E-20
657	2.26962E-20
658	2.0893E-20
659	1.8396E-20
660	1.77725E-20
661	1.69413E-20
662	1.75561E-20
663	1.54074E-20

FIGURE 9. Visible Transmittance Spectrum of CClF2NO at 243 K. Pathlength = 9 cm, Pressure = 100 torr (approximate).

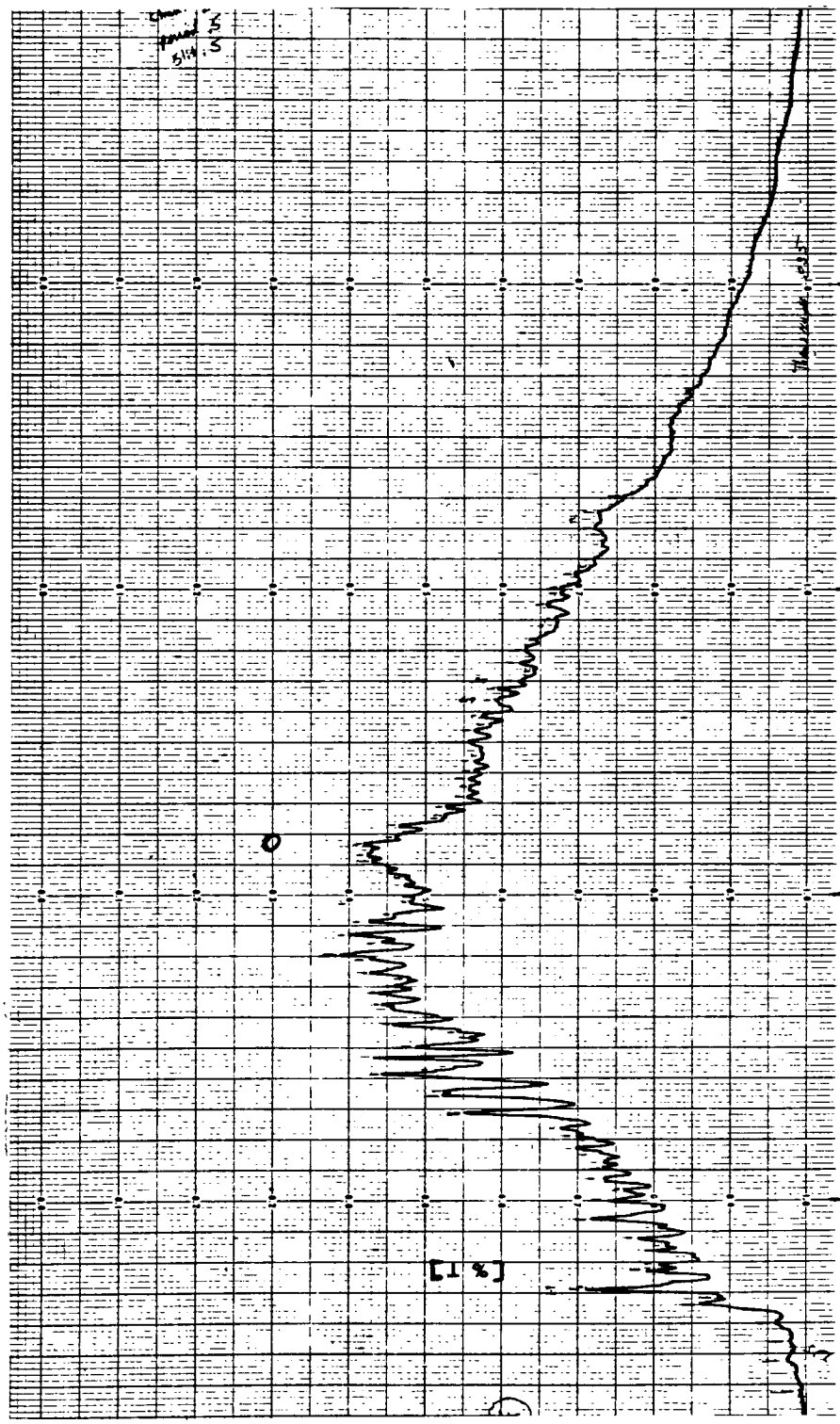

FIGURE 10. Visible Transmittance Spectrum of CCl2FNO at 243 K. Pathlength = 9 cm., pressure = 100 torr (approximate).

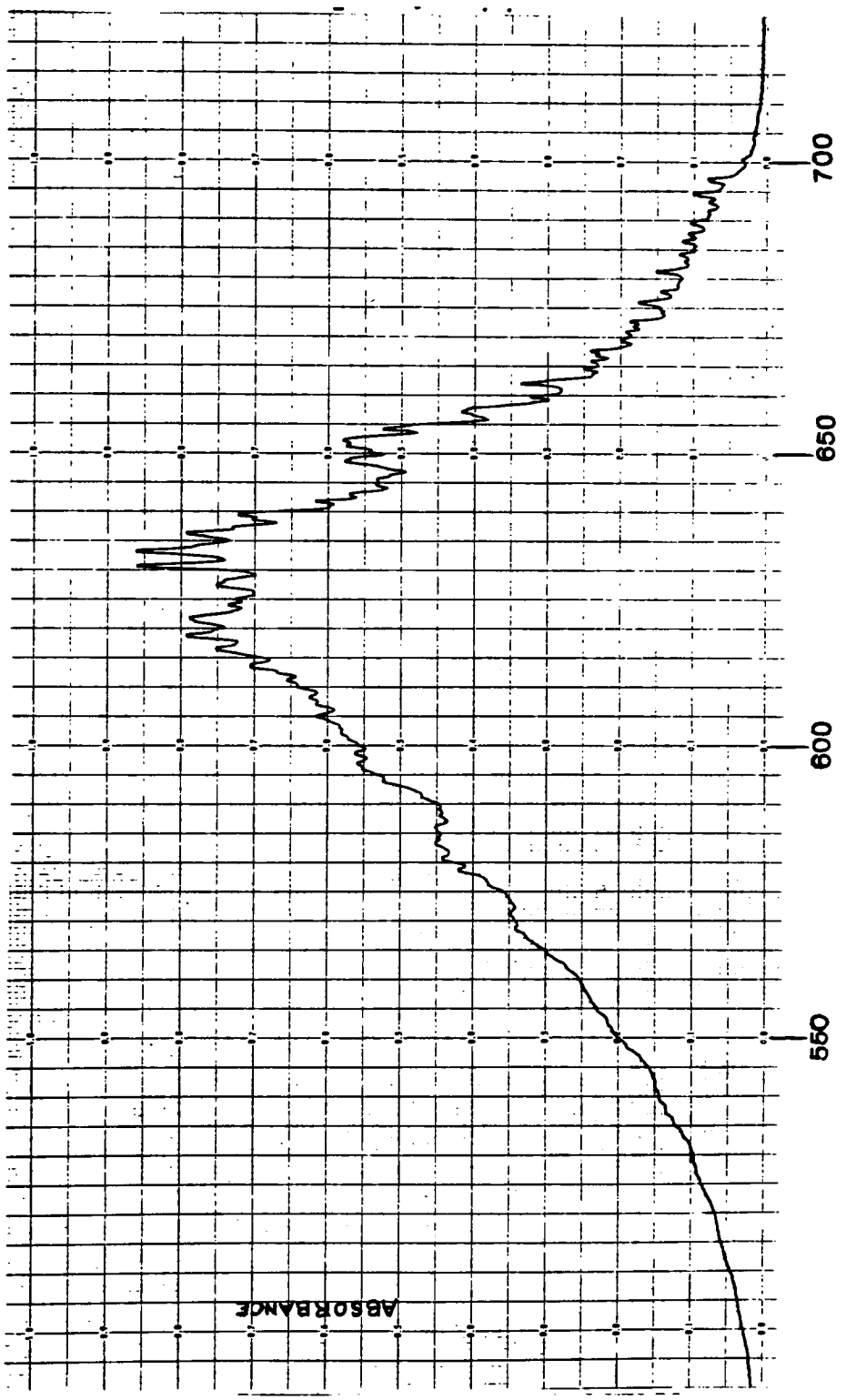

TABLE 6

Wavelengths of the Individual Peaks in the Visible Absorption Spectrum of CClF2NO at 243 K.

Wavelength (nm) ±0.1 nm				
731.3	696.3	668.5	642.5	615.0
728.1	694.5	667.9	641.5	613.3
726.0	693.4	666.0	640.4	612.0
722.9	691.3	664.8	638.5	610.0
719.9	689.8	663.6	637.3	609.6
716.7	689.3	662.7	636.8	608.2
715.6	688.1	660.4	635.4	605.7
714.3	685.5	659.8	633.8	604.6
711.3	682.6	657.6	632.5	602.4
710.2	682.1	656.4	629.4	600.5
708.0	679.2	654.2	628.0	599.7
707.1	678.7	653.3	627.2	597.4
706.0	678.2	651.0	626.2	596.7
704.2	676.6	650.3	624.8	595.2
702.9	674.8	648.3	622.9	592.6
700.9	673.3	647.1	622.1	590.9
699.9	672.2	646.1	620.6	589.8
698.2	671.1	644.3	618.1	588.2
696.7	669.8	643.3	616.2	584.8

TABLE 7

Wavelengths of the Individual Peaks in the Visible Absorption Spectrum of CCl2FNO at 243 K.

Wavelength (nm) ±0.1 nm				
700.6	671.0	636.3	594.0	552.4
698.3	669.4	633.2	691.5	550.6
697.2	667.7	630.6	589.2	548.9
696.9	667.0	628.2	588.2	545.9
694.7	665.9	627.4	586.1	545.0
693.4	664.6	626.1	584.3	543.6
693.1	663.7	625.0	583.3	542.1
691.7	662.1	624.1	580.7	540.5
691.0	661.0	621.8	578.7	539.8
689.6	659.8	618.8	576.8	537.3
687.8	657.3	616.5	576.3	535.6
687.5	654.2	613.6	574.3	533.8
686.5	652.3	612.8	573.4	531.8
685.2	651.4	611.3	572.9	531.2
684.3	650.3	610.2	571.3	529.2
683.1	648.7	608.4	570.3	527.0
681.4	646.2	607.1	568.7	525.6
679.5	645.5	605.1	567.2	523.2
679.2	644.7	603.3	565.0	522.0
677.9	643.1	602.1	564.7	521.3
676.1	641.8	601.3	562.3	520.0
675.0	641.0	600.1	561.8	519.3
674.3	639.5	598.8	560.1	518.5
672.7	638.8	597.1	556.5	517.3
671.9	637.3	596.2	555.0	

The ultraviolet absorption spectra of CClF2NO and CCl2FNO possess a strong absorption band together with a weak shoulder appearing between 260 and 320 nm. Similar absorption was reported for other geminal chloro-nitroso compounds 2-chloro-2-nitroso-propane, 2-chloro-2-nitroso-butane, 1-chloro-1-nitrosocyclohexane and 2,2-dimethyl-3-chloro-3-nitrosobutane [41]. The shoulder becomes more prominent along the series beginning with CCl3NO [1] and continuing down the line of decreasing chlorine atoms with CCl2FNO and CClF2NO to CF3NO [1]. The shoulder has been assigned to an n -- π^* transition of oxygen non- bonding electrons for CF3NO [42]. The more intense short wave length band arises from a π -- π^* transition [42].

The photolysis of carbon-nitrosoalkane bonds upon absorption of red light in the region of 586 to 680 nm causes C-N bond rupture [41], see reaction (12), as has been demonstrated in the photodissociation of CCl3NO [43] and CF3NO [44].

$$RNO + h\nu \longrightarrow R + NO \qquad (12)$$

If the C-N bond strengths for CClF2NO and CFCl2NO are assumed to be 31 ±3 kcal/mole and 32 ±3 kcal/mole as they are for CF3NO and CCl3NO, respectively [45], reaction (15) is energetically possible at wavelengths less than 922 and 893 nm, respectively. Using these bond energies and the heats of formation for CF3 [46], CF2Cl [47], CFCl2 [47], CCl3 [46,48] and NO [46], the heats of formation of CF3NO, CClF2NO, CCl2FNO and CCl3NO were calculated to be -122 ±4, -74 ±5, -33 ±7 and -9 ±4 kcal/mole, respectively, at 298 degrees Kelvin.

$$CX_3NO_2 + h\nu \longrightarrow CX_2O + XNO \qquad (15)$$

B. CHLORODIFLUORONITROMETHANE AND DICHLOROFLUORONITROMETHANE

1) Preparation and Purity

Early attempts by others to prepare $CClF_2NO_2$ and CF_3NO_2 in the laboratory by the oxidation of their corresponding nitrosomethane analogs with dimanganese heptoxide, lead dioxide and chromic oxide resulted in poor yields [9,21]. The low yields (less than 12 percent) were attributed to extensive decomposition of the parent compounds.

Subsequent work had shown that greater yields are obtainable for CF_3NO_2 using the milder oxidizing agent, hydrogen peroxide [13,21]. In the present study, reaction (13) was utilized in the synthesis of the nitro compounds, $CClF_2NO_2$ and CCl_2FNO_2.

$$CX_3NO + H_2O_2 \longrightarrow CX_3NO_2 + H_2O \qquad (13)$$

Infrared spectra of samples taken during the purification of both nitro compounds were observed for any changes in peak intensities due to the removal of impurities. More specifically, this involved comparing the IR spectrum of the original compound to spectra of fractions taken between bulb-to-bulb distillations. Impurities isolated by this method had vapor pressures sufficiently different from the bulk of the material so that their concentration, relative to the main product, changed during the distillation process. The impurities were therefore discernable as fluctuating peaks among the main spectrum of the compound. This method worked well in obtaining the final compounds used in this work. The following is an example of how this technique was applied.

Final purification of CClF2NO2 by distillation was achieved by the reduction of an unknown impurity possessing an IR absorption band at 1760 cm-1 as shown in Figure 11. Therefore, monitoring the peak at 1760 cm-1 assisted in optimizing the samples purity by means of distillation.

UV-Vis scans of the CCL2FNO2 product obtained from the oxidation of CCl2FNO showed the presence of trace NO2-N2O4 in the sample. The NO2-N2O4 may be formed as a decomposition by-product particularly if the system had not originally been oxygen free. The NO2-N2O4 impurity was removed by passing the crude product through a column of CaCl2, as outlined in the experimental section. The NO2- N2O4 was converted to ClNO, as in reaction (13) [33].

$$2NO_2 + 1/2\ CaCl_2 \longrightarrow ClNO + 1/2\ Ca(NO_3)_2 \qquad (13)$$

The ClNO was removed from the CCl2FNO2 product by distillation at the temperature of a dry-ice and acetone slush bath. The volatile fraction was discarded.

The vapor pressures for CClF2NO2 and CCl2FNO2 were measured at four temperatures (see Table 3) ranging from 0 to -63 degrees Celsius. A plot of this data is shown in Figure 12 and the following linear equations were obtained for CClF2NO2 and CCl2FNO2, respectively, using the method of least-squares to fit the data:

$$\ln P\ (\text{torr}) = 16.92 - 3059/T\ (\text{K})$$

$$\ln P\ (\text{torr}) = 17.97 - 3822/T\ (\text{K})$$

Extrapolation of the vapor pressure curves gave boiling points of 24 degrees Celsius (as compared to the previously reported value of 25 degrees Celsius [9]) and 64 degrees Celsius for CClF2NO2 and CCl2FNO2 respectively. Using the Clausius Clapeyron equation, the heats of vaporization for CClF2NO2 and CCl2FNO2 were calculated to be 6.1 kcal/mole and 7.6 kcal/mole, respectively.

FIGURE 11. Infrared Spectrum of CC12FNO2
Showing the Impurity at 1760 cm-1

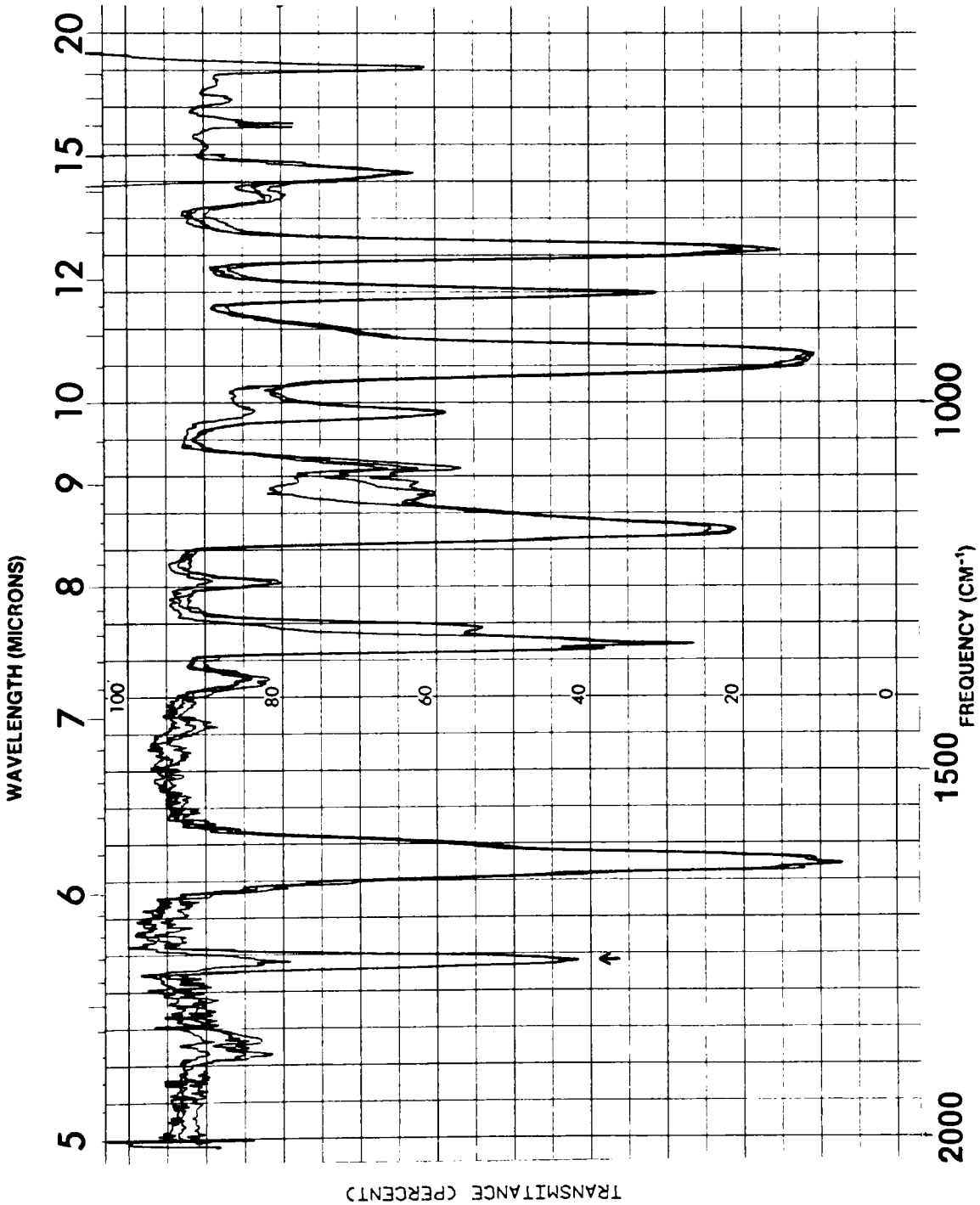

FIGURE 12. Temperature Dependence of the Vapor Pressure of CClF2NO2 and CCl2FNO2

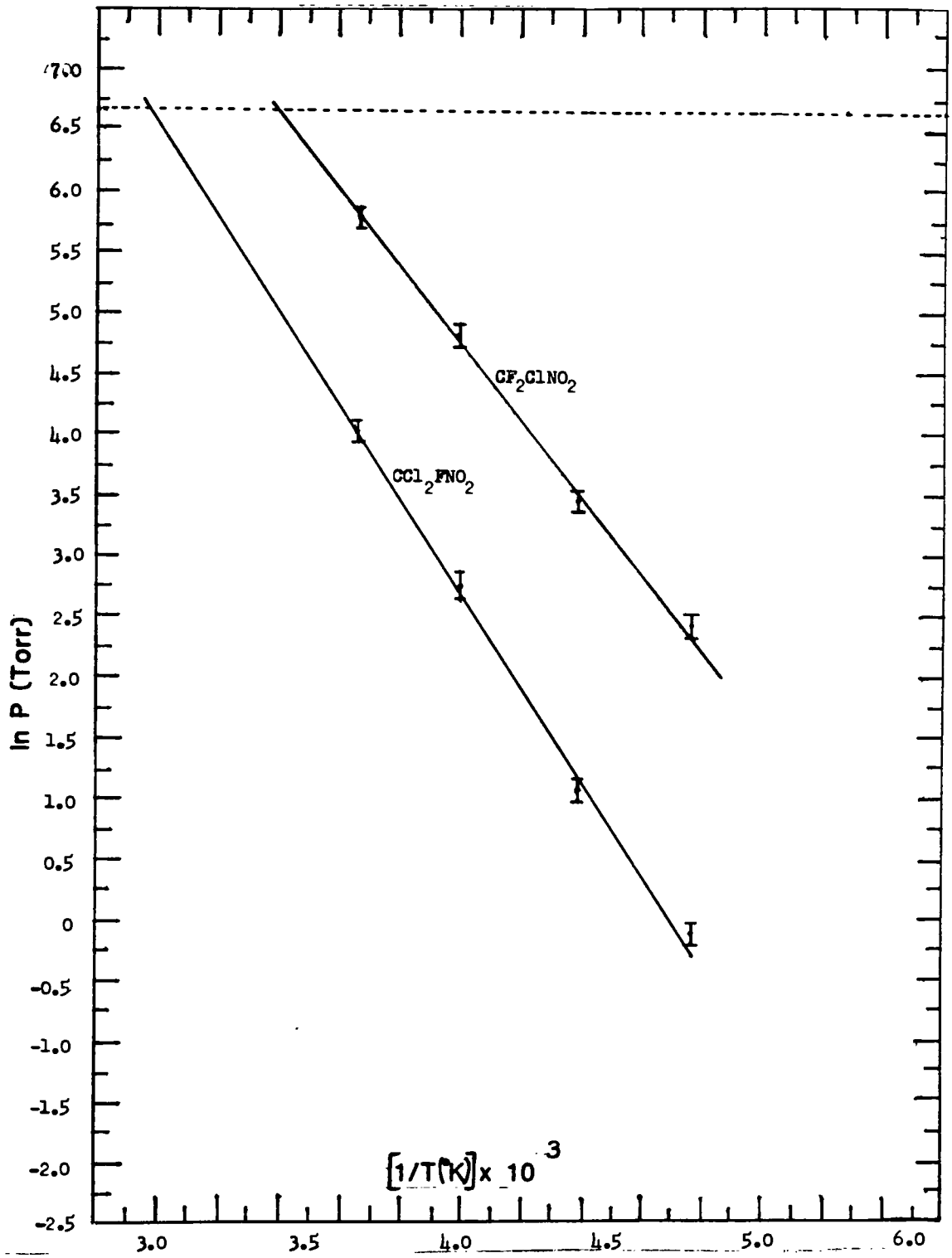

2. The IR Absorption Spectra of CClF2NO2 and CCl2FNO2

The infrared absorption spectra of CClF2NO2 and CCl2FNO2 are shown in Figures 13 and 14, respectively. The fundamental vibrational modes of CClF2NO2 and CCl2FNO2 were assigned using the information obtained from infrared absorption studies of CF3NO2 [36], CCl3NO2 [36], CClF2NO [23] and CCl2FNO (see Table 8). A complete interpretation of the vibrational spectra of CClF2NO2 and CCl2FNO2 can be expected to be more complicated than for CF3NO2 and CCl3NO2 because of the presence of a greater number of stable rotational conformeres in the mixed halogen compounds [49]. The symmetric C-N stretching modes were assigned frequencies consistant with analogous stretching modes reported for CF3NO2 and CCl3NO2. The frequencies that have been reported for the C-N symmetric stretches of CF3NO, CClF2NO, CCl2FNO and CCl3NO are 810 cm-1 [28,21], 768 cm-1 [23], 943 cm-1 [23] and 936 cm-1 [23], respectively. The C-N symmetric stretch of CClF2NO appears to be incorrectly assigned and the correct assignment could possibly be the sharp band at 925 cm-1 or the previously unassigned peak at 985 cm-1 [23].

The NO2 deformation frequencies of CClF2NO2 and CCl2FNO2 (see Table 8) falls on the straight line relationship between the deformation frequency and the electronegativity of X in CX3NO2 when X=H, Br, Cl and F [36]. The remaining observed peaks that have been left unassigned are located at 654 (w), 882 (w), 983 (s), 1030 (w), 2480 (w), 2650 (w) and 2930 cm-1 (w) for CClF2NO2 and 725 (w), 934 (s), 1015 (w), 1090 (w), 1380 (w), 1760 (w) and 2645 cm-1 (w) for CCl2FNO2.

3. The Absorption Cross-Sections of CClF2NO2 and CCl2FNO2

The computer-averaged spectra of CClF2NO2 and CCl2FNO2 are shown in Figures 15 and 16, respectively. The cross-section data for the plots shown in figures 15 and 16 is given in Tables 9 and 10, respectively. The spectra were obtained from scans taken over a range of pressures from 0.1 to 86 torr for CClF2NO2 and 0.2 to 60 torr for CCl2FNO2 and averaged with the aid of an Imsai 8080 microcomputer that was interfaced to the Cary-219 UV-Vis spectrophotometer. A constant spectral bandwidth of 1 nm was maintained throughout all scans.

FIGURE 13. Infrared Spectrum of CClF2NO2 at 298 K. Pressure = 8 Torr, Pathlength = 10 cm.

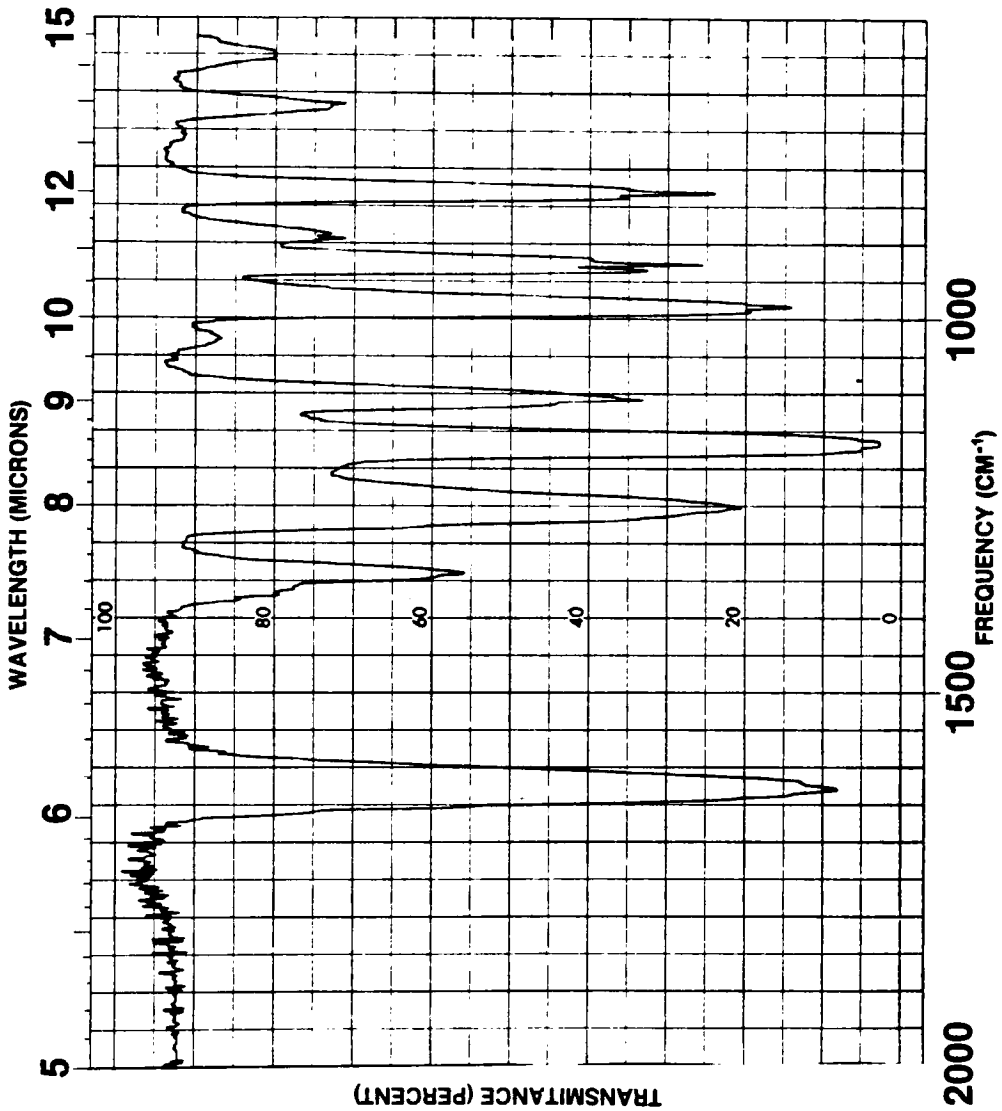

FIGURE 14. Infrared Spectrum of CCl2FNO2 at 298 K. Pressure = 8 Torr, Pathlength = 10 cm.

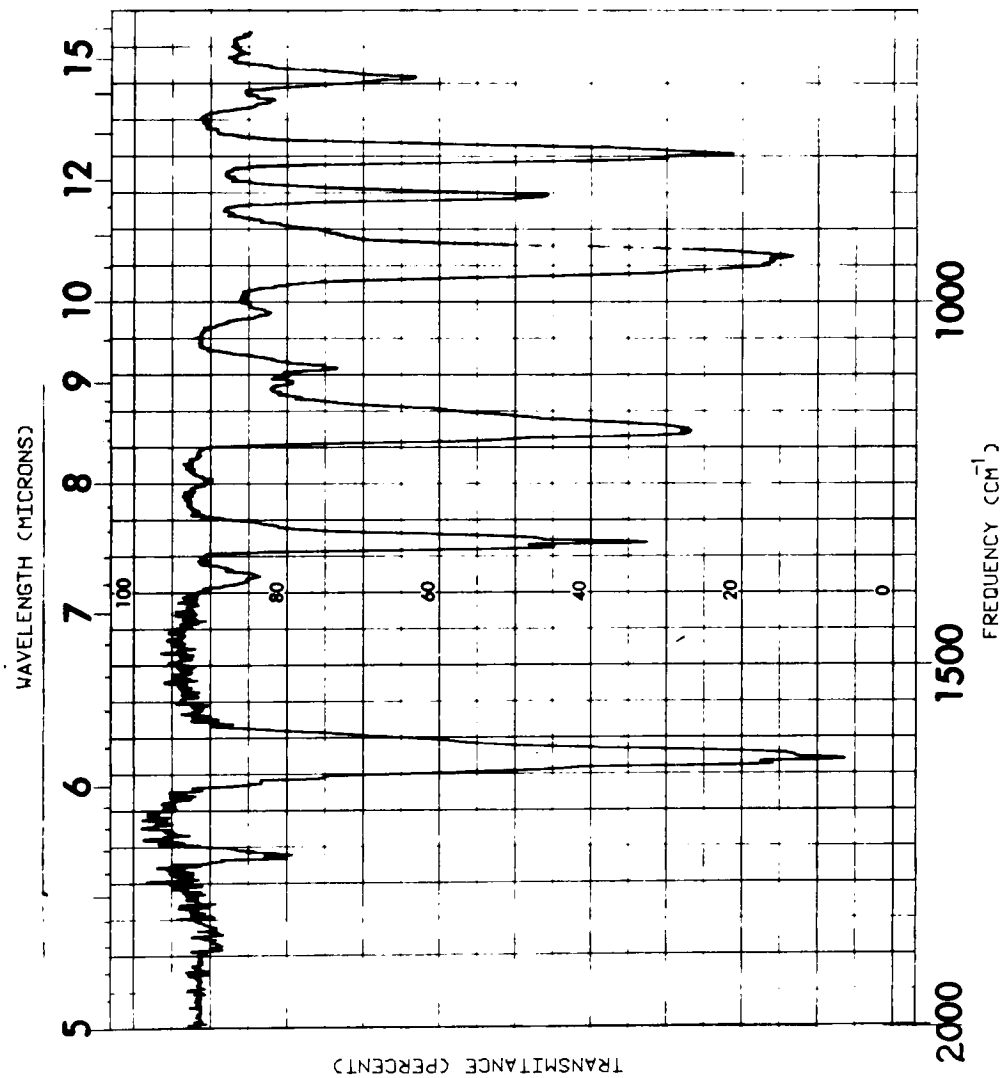

TABLE 8

Observed Frequencies in Wavenumbers and Tentative Band Assignments for Some Halogen-Substituted Methyl Nitrogen Oxides

VIBRATIONAL MODE	CF_3NO	CCl_3NO	$CClF_2NO$	CCl_2FNO	$CClF_2NO_2$	CCl_2FNO_2
NO ASYM STR	1620	1625	1600.5	1614	1628	1628
NO SYM STR	1310	1311	--	--	1338	1329
CF SYM STR	1151	--	1176 1167.5 1149 1087	1147.5 1139.5 1137	1167 1107	1173
CN SYM STR	860	850	768	943	832	850
NO SYM DEF	750	677	--	--	713	690
(a') ($ClCF_2$)	--	--	932 925	--	934 928	--
(a'') ($ClCCl$)	--	--	--	829 823	--	794
(a') (CF_2Cl)	--	--	1243.5	--	1250	--

a Ref. 35
b Ref. 23
c This work.
d See text for discussion of this assignment.

The two prominant absorption maxima that compose the spectrum of both CCl2FNO2 and CClF2NO2 are also found in the analogous spectra of CH3NO2 [34] and CCl3NO2 [35]. The long-wavelength band has been assigned to a n -- π^*transition involving non-bonding oxygen electrons and the short-wavelength band resulting from a π -- π^*transition [34]. A comparison between the peak maxima and minima in the cross-sections of CF3NO2, CClF2NO2, CCl2FNO2 and CCl3NO2 is given in Table 11.

FIGURE 15 UV-Vis Absorption Spectrum of Gaseous CClF2NO2 at 298 K.

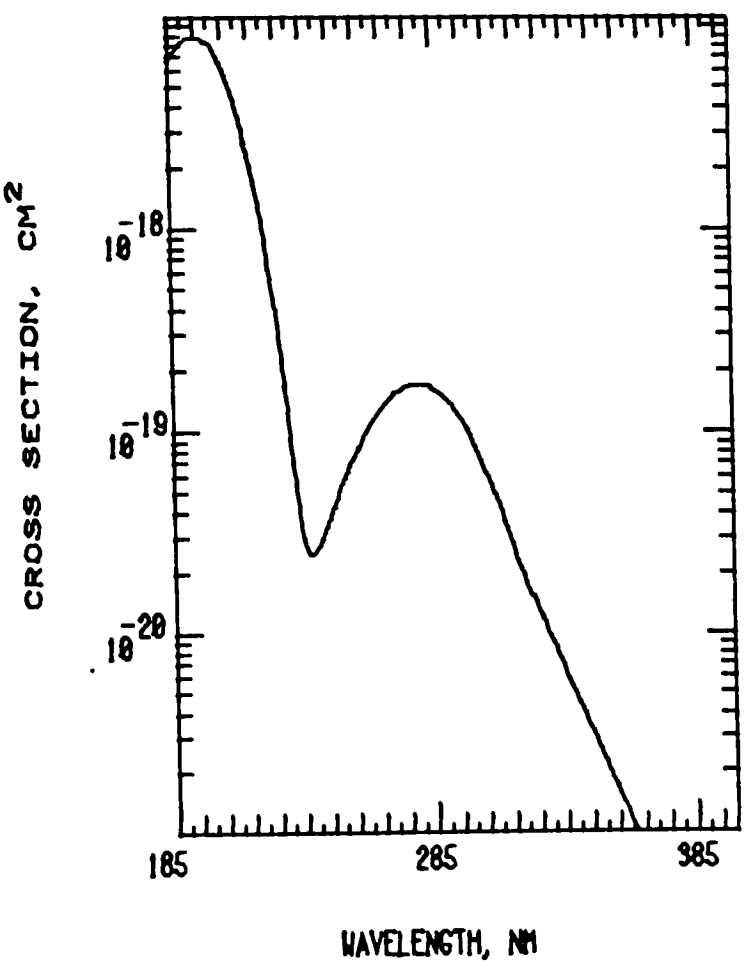

FIGURE 16. UV-Vis Absorption Spectrum of Gaseous CCl2FNO2 at 298 K.

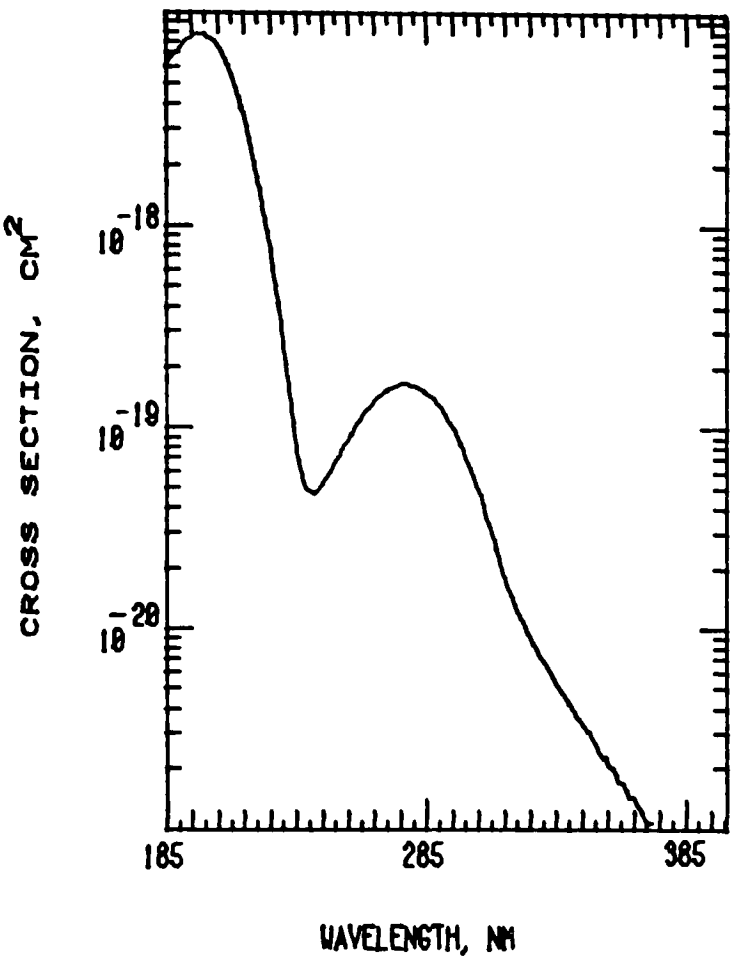

TABLE 9. Averaged Cross-Section Data for $CClF_2NO_2$ Wavelength (nm), Cross-Section (σ), Inherent Error (ξ)[a]

λ	σ	ξ	λ	σ	ξ	λ	σ	ξ
185	1.59E-19	6.61E-18	236	6.76E-22	2.61E-20	287	4.01E-21	1.56E-19
186	1.67E-19	6.99E-18	237	6.47E-22	2.47E-20	288	3.94E-21	1.53E-19
187	1.74E-19	7.33E-18	238	6.41E-22	2.44E-20	289	3.85E-21	1.49E-19
188	1.82E-19	7.67E-18	239	6.52E-22	2.49E-20	290	3.47E-21	1.44E-19
189	1.89E-19	7.99E-18	240	6.75E-22	2.61E-20	291	3.36E-21	1.39E-19
190	1.95E-19	8.27E-18	241	7.10E-22	2.77E-20	292	3.25E-21	1.34E-19
191	2.01E-19	8.50E-18	242	7.53E-22	2.97E-20	293	3.12E-21	1.28E-19
192	2.05E-19	8.70E-18	243	8.01E-22	3.21E-20	294	2.99E-21	1.22E-19
193	2.08E-19	8.85E-18	244	8.57E-22	3.47E-20	295	2.86E-21	1.17E-19
194	2.11E-19	8.95E-18	245	9.18E-22	3.77E-20	296	2.75E-21	1.11E-19
195	2.11E-19	8.98E-18	246	9.83E-22	4.08E-20	297	2.65E-21	1.07E-19
196	2.11E-19	8.97E-18	247	1.05E-21	4.40E-20	298	2.54E-21	1.02E-19
197	2.09E-19	8.88E-18	248	1.26E-21	4.82E-20	299	2.42E-21	9.61E-20
198	2.06E-19	8.76E-18	249	1.35E-21	5.20E-20	300	2.17E-21	8.94E-20
199	2.02E-19	8.57E-18	250	1.43E-21	5.59E-20	301	2.03E-21	8.30E-20
200	1.97E-19	8.34E-18	251	1.52E-21	6.00E-20	302	1.90E-21	7.69E-20
201	1.91E-19	8.05E-18	252	1.62E-21	6.43E-20	303	1.77E-21	7.14E-20
202	1.84E-19	7.72E-18	253	1.72E-21	6.87E-20	304	1.66E-21	6.65E-20
203	1.76E-19	7.36E-18	254	1.82E-21	7.33E-20	305	1.57E-21	6.23E-20
204	1.67E-19	6.95E-18	255	1.92E-21	7.80E-20	306	1.49E-21	5.84E-20
205	1.57E-19	6.52E-18	256	2.03E-21	8.31E-20	307	1.40E-21	5.43E-20
206	1.47E-19	6.07E-18	257	2.14E-21	8.80E-20	308	1.31E-21	5.02E-20
207	1.38E-19	5.62E-18	258	2.37E-21	9.41E-20	309	9.73E-22	4.76E-20
208	1.27E-19	5.15E-18	259	2.48E-21	9.92E-20	310	8.96E-22	4.33E-20
209	1.17E-19	4.68E-18	260	2.60E-21	1.04E-19	311	8.26E-22	3.95E-20
210	1.07E-19	4.22E-18	261	2.72E-21	1.10E-19	312	7.63E-22	3.60E-20
211	9.73E-20	3.78E-18	262	2.83E-21	1.15E-19	313	7.06E-22	3.29E-20
212	6.17E-20	3.53E-18	263	2.94E-21	1.20E-19	314	6.54E-22	3.00E-20
213	5.52E-20	3.11E-18	264	3.05E-21	1.25E-19	315	6.07E-22	2.75E-20
214	4.90E-20	2.71E-18	265	3.16E-21	1.30E-19	316	5.65E-22	2.52E-20
215	4.32E-20	2.33E-18	266	3.26E-21	1.35E-19	317	5.27E-22	2.31E-20
216	3.80E-20	1.99E-18	267	3.37E-21	1.40E-19	318	4.92E-22	2.11E-20
217	3.34E-20	1.69E-18	268	3.47E-21	1.44E-19	319	4.60E-22	1.94E-20
218	2.56E-20	1.56E-18	269	3.86E-21	1.50E-19	320	4.32E-22	1.79E-20
219	2.16E-20	1.30E-18	270	3.95E-21	1.53E-19	321	4.05E-22	1.64E-20
220	1.81E-20	1.06E-18	271	4.03E-21	1.57E-19	322	3.82E-22	1.51E-20
221	1.51E-20	8.61E-19	272	4.11E-21	1.60E-19	323	2.62E-22	1.51E-20
222	1.25E-20	6.91E-19	273	4.17E-21	1.63E-19	324	2.47E-22	1.40E-20
223	1.04E-20	5.51E-19	274	4.23E-21	1.65E-19	325	2.33E-22	1.29E-20
224	8.67E-21	4.34E-19	275	4.28E-21	1.68E-19	326	2.20E-22	1.20E-20
225	9.42E-21	3.91E-19	276	4.33E-21	1.70E-19	327	2.08E-22	1.11E-20
226	7.33E-21	3.00E-19	277	4.35E-21	1.71E-19	328	1.97E-22	1.03E-20
227	4.75E-21	2.23E-19	278	4.36E-21	1.71E-19	329	1.87E-22	9.57E-21
228	3.63E-21	1.67E-19	279	4.36E-21	1.71E-19	330	1.78E-22	8.90E-21
229	2.78E-21	1.25E-19	280	4.36E-21	1.71E-19	331	1.70E-22	8.26E-21
230	2.15E-21	9.38E-20	281	4.35E-21	1.71E-19	332	1.62E-22	7.70E-21
231	1.69E-21	7.11E-20	282	4.33E-21	1.70E-19	333	1.55E-22	7.17E-21
232	1.36E-21	5.46E-20	283	4.30E-21	1.68E-19	334	1.48E-22	6.68E-21
233	9.94E-22	4.13E-20	284	4.25E-21	1.66E-19	335	1.42E-22	6.23E-21
234	8.37E-22	3.38E-20	285	4.18E-21	1.63E-19	336	1.36E-22	5.81E-21
235	7.36E-22	2.90E-20	286	4.09E-21	1.60E-19	337	1.31E-22	5.42E-21

[a] See Appendix I

λ	σ	ε
338	1.26E-22	5.07E-21
339	1.22E-22	4.74E-21
340	1.18E-22	4.43E-21
341	1.14E-22	4.15E-21
342	1.10E-22	3.85E-21
343	1.07E-22	3.60E-21
344	1.03E-22	3.37E-21
345	1.00E-22	3.13E-21
346	9.74E-23	2.93E-21
347	9.49E-23	2.74E-21
348	9.26E-23	2.57E-21
349	8.99E-23	2.37E-21
350	8.78E-23	2.21E-21
351	8.58E-23	2.06E-21
352	8.39E-23	1.93E-21
353	8.22E-23	1.80E-21
354	8.08E-23	1.69E-21
355	7.91E-23	1.57E-21
356	7.76E-23	1.46E-21
357	7.65E-23	1.38E-21
358	7.51E-23	1.28E-21
359	7.38E-23	1.18E-21
360	7.29E-23	1.11E-21
361	7.18E-23	1.03E-21
362	7.08E-23	9.57E-22
363	6.99E-23	8.87E-22
364	6.89E-23	8.13E-22
365	6.82E-23	7.62E-22
366	6.75E-23	7.11E-22
367	6.68E-23	6.59E-22
368	6.61E-23	6.12E-22
369	6.56E-23	5.72E-22
370	6.50E-23	5.24E-22
371	6.44E-23	4.84E-22
372	6.41E-23	4.59E-22
373	6.35E-23	4.19E-22
374	6.31E-23	3.90E-22
375	6.28E-23	3.68E-22
376	6.26E-23	3.54E-22
377	6.20E-23	3.06E-22
378	6.16E-23	2.77E-22
379	6.17E-23	2.81E-22
380	6.15E-23	2.67E-22
381	6.12E-23	2.49E-22
382	6.09E-23	2.27E-22
383	6.07E-23	2.12E-22
384	6.07E-23	2.09E-22
385	6.04E-23	1.87E-22
386	6.01E-23	1.66E-22
387	6.00E-23	1.58E-22
388	5.99E-23	1.47E-22
389	5.98E-23	1.44E-22
390	5.97E-23	1.33E-22
391	5.97E-23	1.33E-22
392	5.95E-23	1.22E-22
393	5.93E-23	1.04E-22
394	5.91E-23	9.34E-23
395	5.93E-23	1.08E-22
396	5.92E-23	9.71E-23
397	5.90E-23	8.27E-23
398	5.91E-23	9.34E-23
399	5.89E-23	7.91E-23
400	5.91E-23	9.34E-23

TABLE 10. Averaged Cross-Section Data for CC12FNO2 Wavelenth (nm), Cross-Section (σ), Inherent Error (ξ) [a]

λ	σ	ξ
185	1.55E-19	6.21E-18
186	1.60E-19	6.42E-18
187	1.65E-19	6.64E-18
188	1.70E-19	6.88E-18
189	1.76E-19	7.14E-18
190	1.82E-19	7.40E-18
191	1.88E-19	7.66E-18
192	1.94E-19	7.91E-18
193	1.99E-19	8.15E-18
194	2.04E-19	8.37E-18
195	2.08E-19	8.55E-18
196	2.11E-19	8.67E-18
197	2.13E-19	8.76E-18
198	2.14E-19	8.79E-18
199	2.14E-19	8.78E-18
200	2.12E-19	8.71E-18
201	2.09E-19	8.59E-18
202	2.05E-19	8.41E-18
203	2.00E-19	8.19E-18
204	1.94E-19	7.91E-18
205	1.87E-19	7.60E-18
206	1.79E-19	7.24E-18
207	1.69E-19	6.84E-18
208	1.60E-19	6.43E-18
209	1.50E-19	5.99E-18
210	1.40E-19	5.55E-18
211	1.30E-19	5.10E-18
212	1.19E-19	4.64E-18
213	1.09E-19	4.18E-18
214	9.92E-20	3.76E-18
215	6.27E-20	3.52E-18
216	5.60E-20	3.10E-18
217	4.96E-20	2.71E-18
218	4.37E-20	2.34E-18
219	3.84E-20	2.01E-18
220	3.37E-20	1.72E-18
221	2.27E-20	1.51E-18
222	1.95E-20	1.26E-18
223	1.66E-20	1.05E-18
224	1.10E-20	9.08E-19
225	9.23E-21	7.43E-19
226	7.79E-21	6.04E-19
227	6.58E-21	4.88E-19
228	9.01E-21	4.05E-19
229	7.33E-21	3.22E-19
230	5.97E-21	2.55E-19
231	5.41E-21	2.00E-19
232	4.36E-21	1.58E-19
233	3.56E-21	1.26E-19
234	2.96E-21	1.03E-19
235	2.41E-21	7.73E-20
236	2.08E-21	6.58E-20
237	1.86E-21	5.78E-20
238	1.71E-21	5.24E-20
239	1.61E-21	4.91E-20
240	1.56E-21	4.73E-20
241	1.54E-21	4.67E-20
242	1.55E-21	4.73E-20
243	1.58E-21	4.82E-20
244	1.62E-21	4.98E-20
245	1.68E-21	5.19E-20
246	1.75E-21	5.43E-20
247	1.82E-21	5.71E-20
248	1.91E-21	6.03E-20
249	2.01E-21	6.37E-20
250	2.10E-21	6.72E-20
251	2.21E-21	7.10E-20
252	2.32E-21	7.49E-20
253	2.43E-21	7.91E-20
254	2.56E-21	8.35E-20
255	2.68E-21	8.80E-20
256	2.50E-21	9.39E-20
257	2.60E-21	9.86E-20
258	2.71E-21	1.03E-19
259	2.82E-21	1.08E-19
260	2.94E-21	1.13E-19
261	3.05E-21	1.18E-19
262	3.16E-21	1.23E-19
263	3.26E-21	1.27E-19
264	3.37E-21	1.32E-19
265	3.47E-21	1.36E-19
266	3.57E-21	1.40E-19
267	3.66E-21	1.44E-19
268	3.75E-21	1.48E-19
269	3.83E-21	1.51E-19
270	3.90E-21	1.54E-19
271	3.96E-21	1.57E-19
272	4.02E-21	1.60E-19
273	4.06E-21	1.62E-19
274	4.10E-21	1.63E-19
275	4.13E-21	1.64E-19
276	4.13E-21	1.65E-19
277	4.13E-21	1.64E-19
278	4.12E-21	1.64E-19
279	4.11E-21	1.63E-19
280	4.08E-21	1.62E-19
281	4.05E-21	1.61E-19
282	4.00E-21	1.59E-19
283	3.94E-21	1.56E-19
284	3.85E-21	1.52E-19
285	3.76E-21	1.49E-19
286	3.67E-21	1.45E-19
287	3.59E-21	1.41E-19
288	3.50E-21	1.37E-19
289	3.39E-21	1.33E-19
290	3.27E-21	1.28E-19
291	3.14E-21	1.22E-19
292	3.00E-21	1.16E-19
293	2.86E-21	1.10E-19
294	2.74E-21	1.05E-19
295	2.62E-21	9.96E-20
296	2.51E-21	9.46E-20
297	2.68E-21	8.87E-20
298	2.53E-21	8.32E-20
299	2.36E-21	7.73E-20
300	2.20E-21	7.14E-20
301	2.04E-21	6.59E-20
302	1.90E-21	6.10E-20
303	1.78E-21	5.67E-20
304	1.67E-21	5.28E-20
305	1.57E-21	4.92E-20
306	1.47E-21	4.55E-20
307	9.40E-22	3.96E-20
308	8.67E-22	3.61E-20
309	8.02E-22	3.29E-20
310	7.41E-22	2.99E-20
311	6.87E-22	2.73E-20
312	6.40E-22	2.51E-20
313	5.96E-22	2.30E-20
314	3.88E-22	1.91E-20
315	3.65E-22	1.77E-20
316	3.44E-22	1.64E-20
317	3.25E-22	1.52E-20
318	3.08E-22	1.41E-20
319	2.92E-22	1.31E-20
320	2.78E-22	1.22E-20
321	2.65E-22	1.14E-20
322	2.54E-22	1.07E-20
323	2.43E-22	1.00E-20
324	2.33E-22	9.44E-21
325	2.25E-22	8.92E-21
326	2.17E-22	8.41E-21
327	2.10E-22	7.95E-21
328	2.02E-22	7.51E-21
329	1.96E-22	7.14E-21
330	1.90E-22	6.75E-21
331	1.85E-22	6.42E-21
332	1.81E-22	6.14E-21
333	1.76E-22	5.85E-21
334	1.70E-22	5.50E-21
335	1.66E-22	5.26E-21
336	1.62E-22	5.01E-21
337	1.58E-22	4.74E-21

[a] See Appendix I

λ	σ	ε
338	1.55E-22	4.57E-21
339	1.52E-22	4.38E-21
340	1.49E-22	4.18E-21
341	1.47E-22	4.02E-21
342	1.43E-22	3.76E-21
343	1.40E-22	3.58E-21
344	1.38E-22	3.45E-21
345	1.35E-22	3.31E-21
346	1.33E-22	3.19E-21
347	1.31E-22	3.05E-21
348	1.30E-22	2.99E-21
349	1.26E-22	2.74E-21
350	1.24E-22	2.62E-21
351	1.23E-22	2.51E-21
352	1.20E-22	2.36E-21
353	1.18E-22	2.26E-21
354	1.19E-22	2.29E-21
355	1.16E-22	2.10E-21
356	1.15E-22	2.02E-21
357	1.15E-22	2.01E-21
358	1.12E-22	1.84E-21
359	1.10E-22	1.71E-21
360	1.09E-22	1.69E-21
361	1.09E-22	1.64E-21
362	1.07E-22	1.56E-21
363	1.06E-22	1.45E-21
364	1.05E-22	1.44E-21
365	1.06E-22	1.45E-21
366	1.03E-22	1.31E-21
367	1.03E-22	1.28E-21
368	1.02E-22	1.22E-21
369	1.01E-22	1.16E-21
370	9.97E-23	1.08E-21
371	9.95E-23	1.07E-21
372	9.99E-23	1.10E-21
373	9.83E-23	9.96E-22
374	9.74E-23	9.39E-22
375	9.82E-23	9.86E-22
376	9.82E-23	9.91E-22
377	9.56E-23	8.24E-22
378	9.48E-23	7.78E-22
379	9.59E-23	8.45E-22
380	9.62E-23	8.61E-22
381	9.49E-23	7.83E-22
382	9.40E-23	7.26E-22
383	9.40E-23	7.26E-22
384	9.45E-23	7.57E-22
385	9.39E-23	7.21E-22
386	9.31E-23	6.69E-22
387	9.32E-23	6.74E-22
388	9.33E-23	6.79E-22
389	9.33E-23	6.84E-22
390	9.28E-23	6.53E-22
391	9.28E-23	6.53E-22
392	9.25E-23	6.33E-22
393	9.10E-23	5.39E-22
394	9.07E-23	5.19E-22
395	9.20E-23	6.02E-22
396	9.13E-23	5.55E-22
397	9.09E-23	5.34E-22
398	9.23E-23	6.17E-22
399	9.12E-23	5.50E-22
400	9.26E-23	6.38E-22

TABLE 11

Photoabsorption Cross-Sections at the Maxima and Minima in the UV Absorption Spectra of Gaseous CX_3NO_2

MOLECULE	MAX,NM	MAX,CM2	MIN,NM	MIN,CM2	REF.
CF_3NO_2	277±2	$(4.3\pm0.3)\times10^{-20}$	250±3	$(3.0\pm0.2)\times10^{-20}$	[b] UNPUBLISHED
	277.5	4.3×10^{-20}	239.5	7.6×10^{-21}	42
	279	4.2×10^{-20}	239	7.6×10^{-21}	13
$CClF_2NO_2$	279±3	$(1.7\pm0.1)\times10^{-19}$	238±1	$(2.4\pm0.1)\times10^{-20}$	THIS WORK
	195±1	$(8.8\pm0.2)\times10^{-18}$			THIS WORK
CCl_2FNO_2	276±3	$(1.7\pm0.1)\times10^{-19}$	241±1	$(4.7\pm0.1)\times10^{-20}$	THIS WORK
	198±1	$(8.8\pm0.2)\times10^{-18}$			THIS WORK
CCl_3NO_2	272±2	$(1.6\pm0.1)\times10^{-19}$	242±2	$(4.9\pm0.2)\times10^{-20}$	[a] 35
	275	7.6×10^{-20}	245	2.7×10^{-20}	13
	202±1	$(9.7\pm0.5)\times10^{-18}$			[a] 35

[a] The cross-section axis in Fig.3 of Ref.(35) is incorrectly labelled and should be a factor of 10 larger.

[b] G.B.Fazekas and G.A.Takacs

Photodecomposition of chloro- and fluoro- substituted nitromethanes can be expected to occur with the breakage of the weakest bond (reaction 14) the C-N bond, as in the photodissociation of CH3NO2 [34].

$$CX_3NO_2 + h\nu \longrightarrow CX_3 + NO_2 \qquad (14)$$

Smaller quantum yields of decomposition may be expected to arise because of reactions (15) and (16) [34].

$$CX_3NO_2 + h\nu \longrightarrow CX_2O + XNO \qquad (15)$$

$$CX_3NO_2 + h\nu \longrightarrow CX_3NO + O \qquad (16)$$

The energetics of reactions (14) thru (16) (see Table 12) are such that the absorption of radiation by CClF2NO2 and CCl2FNO2 is of sufficient energy to permit the photodissociation in reactions (14) thru (16) to occur.

Table 12

Heats of Reaction for
Equations 14,15 and 16 at 298 K.

	Reaction			
CX3NO2	(14)	(15)producing ClNO	(15)producing FNO	(16)
CF3NO2	28	---	-36	70
CClF2NO2	28	-56	-34	-34
CCl2FNO2	28	-47	-25	69
CCl3NO2	28	-39	___	69

a
In kcal mol^{-1}

b
Calculated from the heats of formation for CX3NO2, CF3[46], CClF2[47], CCl2F[47], CCl3[46], NO2[46], CCl2O[46], ClFO[46], FNO[46], ClNO[49], CX3NO[45,c] and O[33,34]. The heats of formation of CX3NO2 were calculated from the bond dissociation energy of X3C-NO2 and the heats of formation of CX3 and NO2. Bond dissociation energies, D, of F3C-NO2 and F2ClC-NO2 were estimated using D(X3C-NO2) = D(X3C-NO) + D(F-NO2) - D(F-NO) while for FCl2C-NO2 and Cl3C-NO2 the equation D(X3C-NO2) = D(X3C-NO) + D(Cl-NO2) - D(Cl-NO) was used. The dissociation energies for X3C-NO were obtained from [45,c] and those for F-NO2, Cl-NO2, F-NO and Cl-NO were calculated from the heats of formation of F[50], Cl[50], NO[46], FNO2[46] and ClNO2[46]. The estimated heats of formation of gaseous CF3NO2, CClF2NO2, CCl2FNO2 and CCl3NO2 at 298 K are -132, -84, -43 and -1 kcal/mol, respectively.

c
This work.

C. The Atmospheric Photochemical Stability of CC1F2NO, CC12FNO, CC1F2NO2 and CC12FNO2

Shown in Table 13 are the Photodissociation rate coefficients (J) and lifetimes (1/J) values for CX3NO and CX3NO2. J values were obtained by the integration of equation (8).

$$J = \int \Phi I \sigma \, d\lambda \qquad (8)$$

The quantum yield for the photodecomposition, Φ, was taken as unity over all the absorbing wavelengths for each compound.

Values for solar flux intensities, I, were obtained from the Lawrence Livermore Laboratory and are given in Table 14. Values for the photoabsorption cross-sections, σ are given in Tables 4 and 5 for CClF2NO and CCl2FNO, and Tables 9 and 10 for CClF2NO2 and CCl2FNO2, respectively. Equation (8) was evaluated with the use of a computer program utilizing the trapezoidal method of integration with a d interval of 1 nm. Solar flux intensities were interpolated from Table 14, when necessary, to obtain an exact wavelength correlation between I values and σ values.

The 1/e photodissociation lifetimes for CClF2NO and CCl2FNO are estimated to be approximately 2 minutes and 1 minute, respectively. The lifetimes are relatively independent of the altitude because CClF2NO and CCl2FNO dissociate primarily by the absorption of intense visible solar radiation [3] where solar flux intensities are nearly constant with altitude.

The fraction 1/e of CClF2NO2 and CCl2FNO2 is estimated to remain after approximately one hour of photodecomposition by sunlight at 30 km. The photochemical stability of CClF2NO2 and CCl2FNO2 may be of greater environmental concern as a potential sink for halogens in contrast to their short lived nitroso analogs. The longer lifetimes of CClF2NO2 and CCl2FNO2 can be attributed to a lack of visible light absorption. However, CClF2NO2 and CCl2FNO2 readily dissociate at higher altitudes upon exposure to shorter wavelengths of radiation characteristic to their absorption spectra.

TABLE 13

Photodissociation Rate Coefficients J and Lifetimes 1/J for CC1F2NO, CC12FNO, CC1F2NO2 and CC12FNO2

ALT. KM	CC1F2NO J,SEC	CC1F2NO 1/J,MIN	CC12FNO J,SEC	CC12FNO 1/J,MIN	CC1F2NO2 J,SEC	CC1F2NO2 1/J,HR	CC12FNO2 J,SEC	CC12FNO2 1/J,HR
0	8.17(-3)	3.0	1.48(-2)	1.1	1.8(-4)	1.5	1.6(-4)	1.7
10	8.38(-3)	2.0	1.53(-2)	1.1	2.6(-4)	1.1	2.3(-4)	1.2
20	8.45(-3)	2.0	1.55(-2)	1.1	2.8(-4)	1.0	2.5(-4)	1.1
30	8.51(-3)	2.0	1.56(-2)	1.1	3.7(-4)	0.8	3.2(-4)	0.9
40	8.55(-3)	1.9	1.59(-2)	1.0	7.7(-4)	0.4	7.2(-4)	0.4
50	8.57(-3)	1.9	1.60(-2)	1.0	1.2(-3)	0.2	1.3(-3)	0.2

TABLE 14. Solar Flux Intensities Used in the Calculation of J Values.

λ	0 km		10 km	20 km	30 km	40 km	50 km
191.3	0.	0.	1.86438E06	3.9284E09	5.3042E10	1.5323E11	
193.6	0.	0.	4.0144E07	1.6053E10	1.30425E11	2.8909E11	
195.9	0.	0.	3.8313E08	5.2033E10	2.9979E11	5.754E11	
117.8	0.	0.	3.3547E08	3.8295E10	2.0232E11	3.6428E11	
199.3	0.	0.	8.7878E08	6.8341E10	2.96655E11	4.9608E11	
201.3	0.	0.	1.8020E09	1.2921E11	5.4519E11	8.3446E11	
203.7	0.	0.	2.3338E09	1.5429E11	6.4234E11	9.7966E11	
205.6	2.9955E-23		9.1036E01	9.1253E08	1.5576E11	9.1771E11	1.2573E12
207.2	9.9556E-22		3.7174E02	2.1938E09	4.3195E11	2.8727E12	3.9983E12
209.4	2.1277E-20		7.0638E02	2.3200E09	5.9848E11	4.8535E12	6.9376E12
211.6	4.7715E-19		6.4386E02	1.0285E09	4.8714E11	5.9045E12	8.9219E12
213.9	4.0837E-18		2.0800E02	1.7753E08	2.5201E11	6.0038E12	9.9796E12
216.2	1.8827E-17		3.3156E01	1.6435E07	1.0958E11	6.5994E12	1.2516E13
218.6	4.4618E-17		2.7772E00	8.4742E05	3.2571E10	5.5561E12	1.2226E13
221.0	3.4626E-17		9.9312E-02	2.2994E04	8.9874E09	5.9276E12	1.5840E13
223.4	4.6099E-18		6.9512E-04	1.5090E02	1.2377E09	4.7156E12	1.6232E13
226.0	1.6135E-19		1.4414E-06	3.5204E-01	1.1181E08	3.4573E12	1.6112E13
228.6	3.3464E-21		1.7731E-09	5.3605E-04	9.6814E06	3.0108E12	1.9605E13
231.2	2.8751E-23		9.0085E-13	3.7043E-07	5.5908E05	2.1686E12	2.0362E13
233.9	6.1805E-26		1.0704E-16	6.9903E-11	1.7978E04	1.2960E12	1.8600E13
236.7	3.5240E-29		3.9956E-21	5.0337E-15	4.0848E02	7.6930E11	1.7741E13
239.5	1.7982E-32		1.1188E-25	2.7323E-19	8.6313E00	4.7914E11	1.8068E13
242.4	3.2905E-34		1.4949E-29	3.6285E-23	2.5674E-01	3.2072E11	1.8975E13
245.4	5.6222E-37		1.3797E-33	5.5615E-27	8.3486E-03	2.1906E11	2.0170E13
248.4	2.5391E-40		8.8524E-37	9.9896E-30	7.2590E-04	1.6494E11	2.0829E13
251.6	3.3615E-42		1.3690E-38	2.7533E-31	1.8301E-04	1.4266E11	2.1577E13
254.8	1.6355E-43		6.4218E-39	1.4682E-31	1.6874E-04	1.7876E11	2.8278E13
258.0	1.0271E-41		3.4367E-38	6.6267E-31	4.3387E-04	3.3699E11	5.0940E13
261.4	5.8009E-38		1.0611E-34	6.0522E-28	4.6289E-03	3.0383E11	3.1989E13
264.9	2.9743E-33		2.8734E-30	4.3734E-24	2.6506E-01	1.1848E12	8.4180E13
268.5	2.7032E-27		1.1266E-24	2.7915E-19	2.1458E01	2.3588E12	9.7439E13
272.1	2.4274E-20		3.8114E-18	1.1026E-13	3.1674E03	4.3417E12	9.4411E13
275.9	5.9396E-13		3.3570E-11	9.9957E-08	6.8778E05	9.1822E12	1.0137E14
279.7	2.1683E-06		4.9825E-05	1.9852E-02	8.8833E07	2.0128E13	1.2238E14
283.7	1.2445E00	1.3080E01	8.9000E02	6.6465E09	4.3184E13	1.5615E14	
287.8	6.3115E04	3.5557E05	5.7700E06	2.5712E11	9.7417E13	2.3244E14	
292.0	7.2927E08	2.4555E09	1.1604E10	6.6147E12	2.2511E14	3.7757E14	
296.3	1.8319E11	4.5069E11	1.0098E12	3.7650E13	2.9060E14	3.9235E14	
300.7	5.0995E12	1.0354E13	1.5462E13	1.0357E14	3.2419E14	3.8370E14	
305.3	4.9776E13	8.9652E13	1.1026E14	2.6071E14	4.6931E14	5.1307E14	
310.0	1.7202E14	2.8765E14	3.2619E14	4.6369E14	6.0612E14	6.3275E14	
315.0	3.3197E14	5.2599E14	5.7423E14	6.5354E14	7.2011E14	7.3201E14	
320.0	5.1022E14	7.7854E14	8.3691E14	8.8978E14	9.2678E14	9.3332E14	
325.0	7.1803E14	1.0618E15	1.1308E15	1.1664E15	1.1862E15	1.1897E15	
330.0	9.5124E14	1.3701E15	1.4512E15	1.4790E15	1.4912E15	1.4934E15	
335.0	9.3647E14	1.3181E15	1.3909E15	1.4095E15	1.4158E15	1.4170E15	
340.0	1.0236E15	1.4114E15	1.4854E15	1.5012E15	1.5057E15	1.5066E15	
345.0	1.1224E15	1.5189E15	1.5952E15	1.6100E15	1.6138E15	1.6145E15	
350.0	1.1649E15	1.5495E15	1.6244E15	1.6383E15	1.6416E15	1.6422E15	
355.0	1.1790E15	1.5439E15	1.6160E15	1.6293E15	1.6324E15	1.6330E15	
360.0	1.2038E15	1.5530E15	1.6230E15	1.6360E15	1.6390E15	1.6396E15	
365.0	1.3783E15	1.7542E15	1.8307E15	1.8450E15	1.8483E15	1.8490E15	
370.0	1.4489E15	1.8206E15	1.8973E15	1.9118E15	1.9152E15	1.9159E15	
375.0	1.4719E15	1.8275E15	1.9020E15	1.9162E15	1.9195E15	1.9202E15	
380.0	1.3978E15	1.7165E15	1.7841E15	1.7972E15	1.8004E15	1.8010E15	
385.0	1.3349E15	1.6221E15	1.6838E15	1.6959E15	1.6988E15	1.6994E15	
390.0	1.3188E15	1.5868E15	1.6450E15	1.6566E15	1.6594E15	1.6600E15	
395.0	1.4484E15	1.7265E15	1.7877E15	1.7999E15	1.8029E15	1.8035E15	
400.0	1.8832E15	2.2258E15	2.3021E15	2.3175E15	2.3213E15	2.3221E15	

405.0	2.3348E15	2.7373E15	2.8278E15	2.8462E15	2.8509E15	2.8518E15
410.0	2.4557E15	2.8573E15	2.9485E15	2.9673E15	2.9721E15	2.9730E15
415.0	2.4662E15	2.8488E15	2.9366E15	2.9548E15	2.9596E15	2.9604E15
420.0	2.5131E15	2.8835E15	2.9692E15	2.9871E15	2.9919E15	2.9927E15
425.0	2.5093E15	2.8608E15	2.9429E15	2.9603E15	2.9650E15	2.9659E15
430.0	2.4307E15	2.7545E15	2.8307E15	2.8470E15	2.8514E15	2.8521E15
435.0	2.4887E15	2.8042E15	2.8790E15	2.8952E15	2.8996E15	2.9004E15
440.0	2.8358E15	3.1782E15	3.2601E15	3.2781E15	3.2831E15	3.2840E15
445.0	3.0204E15	3.3680E15	3.4517E15	3.4704E15	3.4757E15	3.4766E15
450.0	3.1422E15	3.4871E15	3.5707E15	3.5896E15	3.5950E15	3.5960E15
455.0	3.1618E15	3.4930E15	3.5739E15	3.5926E15	3.5980E15	3.5989E15
460.0	3.1528E15	3.4680E15	3.5458E15	3.5647E15	3.5704E15	3.5714E15
465.0	3.1858E15	3.4901E15	3.5656E15	3.5841E15	3.5897E15	3.5907E15
470.0	3.2552E15	3.5524E15	3.6267E15	3.6453E15	3.6511E15	3.6521E15
475.0	3.3359E15	3.6273E15	3.7006E15	3.7197E15	3.7258E15	3.7269E15
480.0	3.3091E15	3.5859E15	3.6563E15	3.6764E15	3.6832E15	3.6843E15
485.0	3.1446E15	3.3965E15	3.4612E15	3.4807E15	3.4875E15	3.4887E15
490.0	3.1254E15	3.3651E15	3.4270E15	3.4458E15	3.4524E15	3.4535E15
495.0	3.2435E15	3.4820E15	3.5440E15	3.5636E15	3.5707E15	3.5719E15
500.0	3.1735E15	3.3976E15	3.4568E15	3.4778E15	3.4859E15	3.4872E15
505.0	3.1770E15	3.3927E15	3.4507E15	3.4743E15	3.4840E15	3.4855E15
510.0	3.1961E15	3.4043E15	3.4605E15	3.4835E15	3.4930E15	3.4946E15
515.0	3.1100E15	3.3047E15	3.3575E15	3.3798E15	3.3890E15	3.3905E15
520.0	3.1079E15	3.2950E15	3.3464E15	3.3696E15	3.3795E15	3.3811E15
525.0	3.2167E15	3.4031E15	3.4551E15	3.4810E15	3.4925E15	3.4943E15
530.0	3.2796E15	3.4628E15	3.5151E15	3.5450E15	3.5589E15	3.5611E15
535.0	3.3526E15	3.5330E15	3.5852E15	3.6170E15	3.6321E15	3.6344E15
540.0	3.3892E15	3.5649E15	3.6163E15	3.6493E15	3.6652E15	3.6676E15
545.0	3.4237E15	3.5947E15	3.6455E15	3.6802E15	3.6971E15	3.6997E15
550.0	3.3981E15	3.5617E15	3.6108E15	3.6458E15	3.6629E15	3.6656E15
555.0	3.3689E15	3.5253E15	3.5730E15	3.6090E15	3.6269E15	3.6297E15
560.0	3.3524E15	3.5030E15	3.5503E15	3.5903E15	3.6107E15	3.6139E15
565.0	3.3514E15	3.4972E15	3.5441E15	3.5877E15	3.6103E15	3.6138E15
570.0	3.3407E15	3.4813E15	3.5276E15	3.5740E15	3.5984E15	3.6022E15
575.0	3.3654E15	3.5022E15	3.5478E15	3.5951E15	3.6201E15	3.6239E15
580.0	3.4007E15	3.5341E15	3.5785E15	3.6242E15	3.6484E15	3.6521E15
585.0	3.4109E15	3.5399E15	3.5829E15	3.6268E15	3.6498E15	3.6534E15
590.0	3.4104E15	3.5352E15	3.5772E15	3.6216E15	3.6450E15	3.6486E15
595.0	3.4179E15	3.5390E15	3.5806E15	3.6265E15	3.6510E15	3.6548E15
600.0	3.4093E15	3.5265E15	3.5676E15	3.6158E15	3.6417E15	3.6457E15
605.0	3.4008E15	3.5138E15	3.5537E15	3.6012E15	3.6268E15	3.6307E15
610.0	3.4016E15	3.5108E15	3.5491E15	3.5937E15	3.6176E15	3.6213E15
615.0	3.4149E15	3.5208E15	3.5576E15	3.5996E15	3.6219E15	3.6254E15
620.0	3.4298E15	3.5324E15	3.5678E15	3.6068E15	3.6273E15	3.6305E15
625.0	3.4304E15	3.5295E15	3.5634E15	3.5995E15	3.6185E15	3.6214E15
630.0	3.4259E15	3.5216E15	3.5543E15	3.5887E15	3.6066E15	3.6094E15
635.0	3.4247E15	3.5172E15	3.5484E15	3.5804E15	3.5970E15	3.5995E15
640.0	3.4298E15	3.5192E15	3.5488E15	3.5769E15	3.5913E15	3.5935E15
645.0	3.4234E15	3.5097E15	3.5383E15	3.5651E15	3.5787E15	3.5808E15
650.0	5.1169E15	5.2418E15	5.2828E15	5.3199E15	5.3386E15	5.3415E15
660.0	6.7924E15	6.9478E15	6.9982E15	7.0413E15	7.0627E15	7.0661E15
670.0	6.7716E15	6.9168E15	6.9631E15	6.9996E15	7.0175E15	7.0203E15
680.0	6.7502E15	6.8859E15	6.9283E15	6.9584E15	6.9728E15	6.9750E15
690.0	6.7080E15	6.8348E15	6.8737E15	6.8989E15	6.9106E15	6.9125E15
700.0	6.6606E15	6.7790E15	6.8149E15	6.8368E15	6.8460E15	6.8476E15
710.0	6.6068E15	6.7175E15	6.7509E15	6.7698E15	6.7783E15	6.7797E15
720.0	6.5552E15	6.6587E15	6.6895E15	6.7055E15	6.7124E15	6.7136E15
730.0	6.5141E15	6.6113E15	6.6399E15	6.6535E15	6.6591E15	6.6601E15

APPENDIX I

Equation Used in the Calculation of Absorption Cross-Sections and Inherent Error in the Cross-Sections

Absorption Cross-Sections, σ values, are a measure of the extent to which molecules absorb radiation. The Cross-Section is defined by the following expression:

$$\sigma = \ln (I_o / I) / C L$$

where C is the concentration in molecules per cm^3, I_o and I are the incident and transmitted radiation, respectively and L is the pathlength in cm.

The inherent errors in the absorption cross-sections, averaged over several cross-section spectra in Tables 9 and 10, are determined by the following expression:

$$d\sigma = (dT + dP + dPL + dA) *$$

where d represents the error in the measurement. The error in the measurements are specified by the user when running the program given in Appendix V which calculates the cross-sections for a stored spectrum.

Typical values entered for the error in measurements are:

dT (temperature) = 1 degree K

dP (pressure) = 0.01 torr

dPL (pathlength) = 0.01 cm

dA (absorbance) is calculated in the program by the following expression:

dA = .0007 * 2.303 / Log (100 / PT)

where PT is the percent transmittance at each wavelength for the compound under study.

APPENDIX II

Software Flow CHart for UV-Vis Data Handling

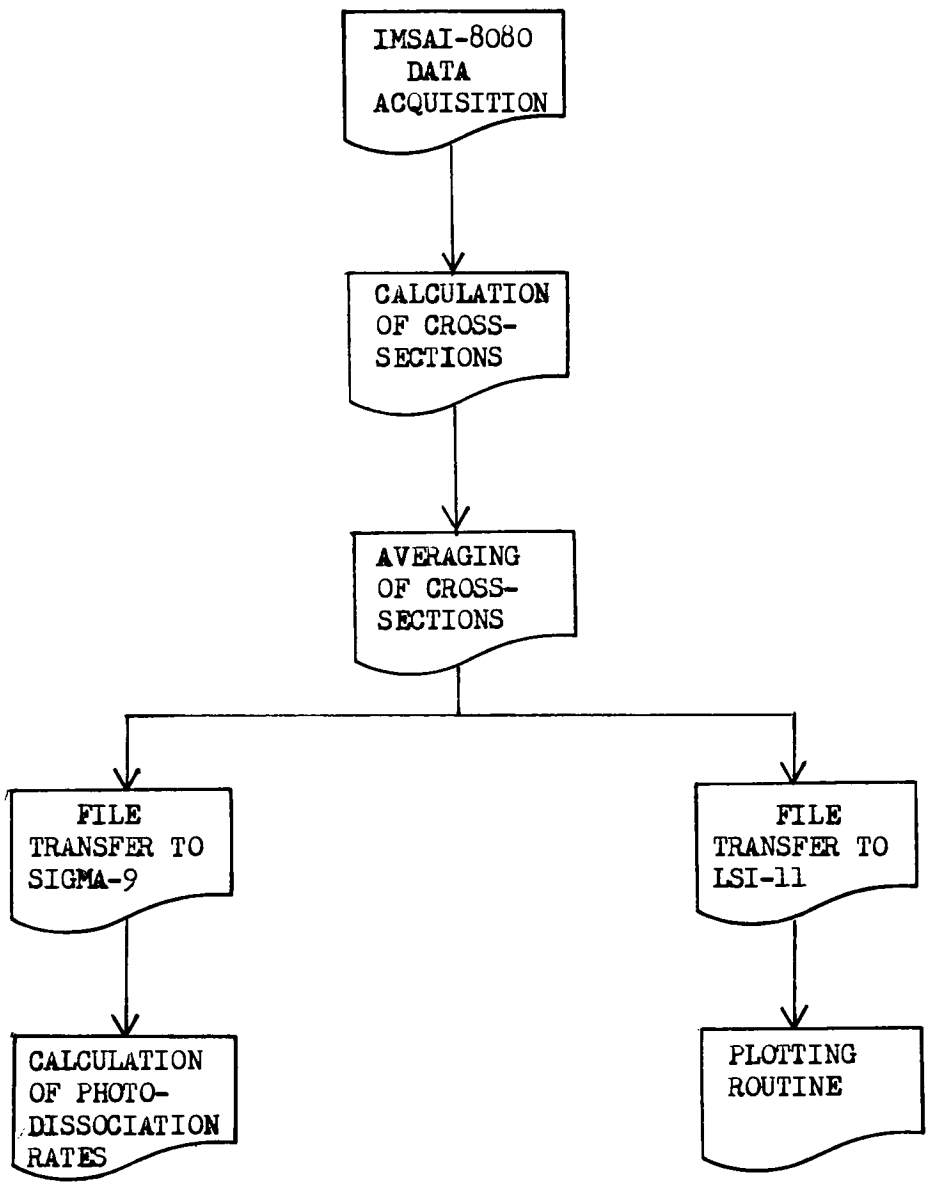

APPENDIX III

Hardware Schematic of Computer Interface

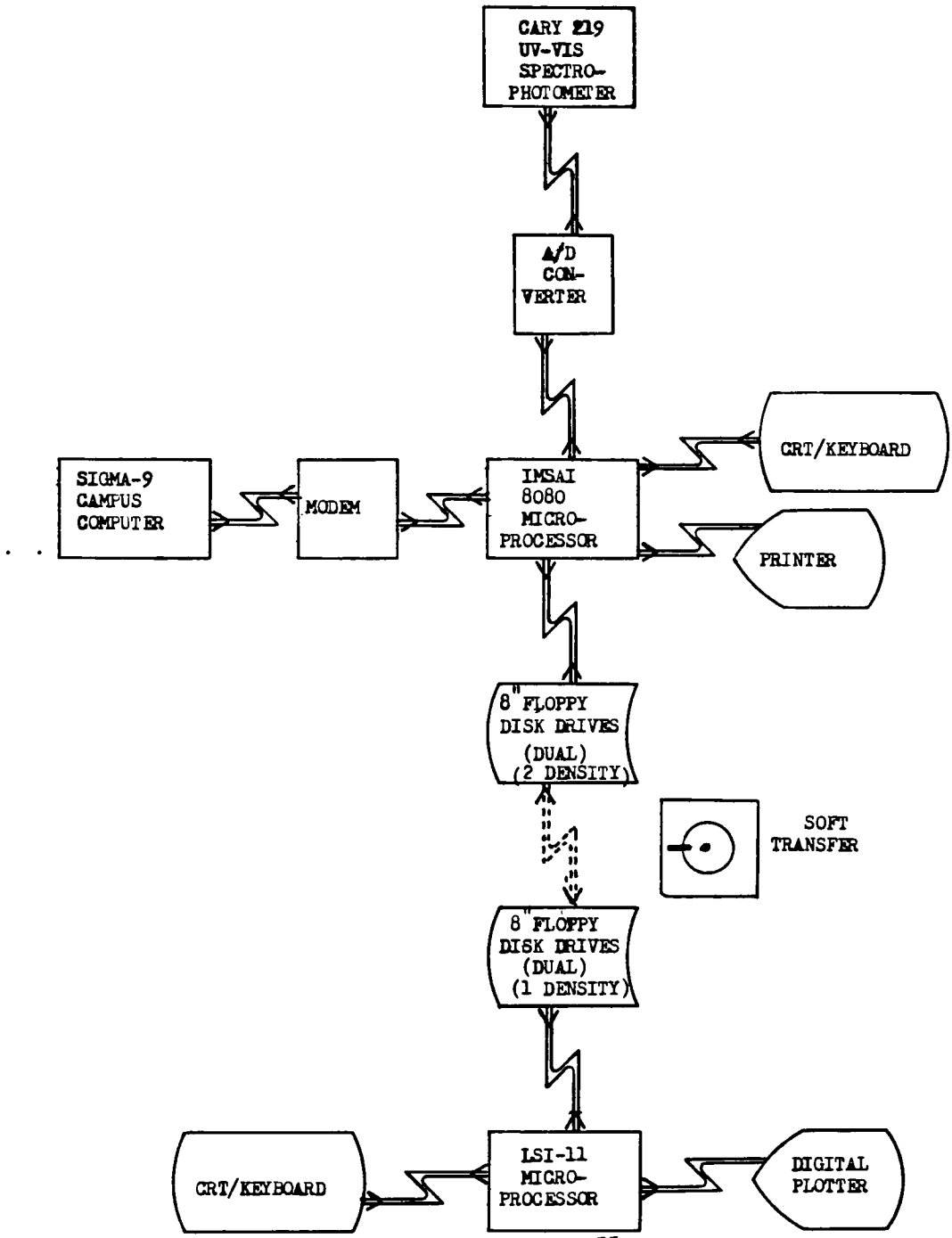

APPENDIX IV

Flow Chart of Program Calls Used for Data Acquisition, Averaging and Plotting
NOTE: CP/M Prompt = A> RT-11 Prompt = .

System	Program Call	Function
8080 CP/M	A >FILES	List Files on Disk A.
	A >RUN C219	Invokes data acquisition routine.
	A >MBASIC CRSC	Invokes program to calculate Cross-Sections.
	A >MBASIC LDISPLAY	Invokes program to output several cross-section data files simultaniously to the printer.
	A >MBASIC DISPLAY	The same as LDISPLAY except that output is directed to the console terminal.
	A >MBASIC AVG	Invokes program to average specified cross-section data files.
	A >MBASIC CHANGE	Invokes program to change a random access data file containing averaged cross-section data to a sequential ASCII file which can be transfered to the LSI-11 for plotting and data handling.
	A >RUN CPMLSI "FILESPEC"	Invokes program which copies specified ASCII data file, "FILESPEC", to an LSI-11 single density disk in drive B.
LSI-11 RT11	.ASS DX1 DK	Assigns disk drive 1 as the default data disk unit.
	.R PIP * .R BASIC * (CR) READY OPEN "FILESPEC" FOR OUTPUT AS FILE #1 CLOSE CTRL C .R PIP *FILESPEC.DAT n =/T	This sequence of commands will create a file to which data may may be transfered to from the 8080 system using the CPMLSI program. The value n must be the integer value of the length of the file in CP/M to be copied divided by 4 plus one.
	.R Basic * (CR) READY OLD"CHANGE" READY RUN	This sequence of commands invokes the program to change the sequential data file transfered form CP/M to a random access file suitabl for plotting.
	OLD"PLOT" ?SYN AT 360	Program to plot data on terminal. This error message occurs while using the PLOT program after the plot has been completed, at this point the program can be reexicuted to overlay another plot or the command GOTO300 will replot the same data on the digital plotter if the plotter is now turned on.

APPENDIX V

CP/M Basic Program to Calculate Photoabsorption Cross-Sections

```
A>MBASOC  COIC CRSC
10 'PROGRAM TO CALCULATE CRSC
20 PRINT "PLEASE ENTER THE DATA FILE NAME"
30 INPUT DFILE$
40 PRINT "TRANSFER FILE NAME"
50 INPUT TFILE$
60 TFILE$="B:"+TFILE$
70 PRINT "TEMPERATURE";
80 INPUT T
90 PRINT "ERROR IN TEMP";
100 INPUT DT
110 PRINT "PRESSURE";
120 INPUT P
130 PRINT "ERROR IN PRES";
140 INPUT DP
150 PRINT "PATHLENGTH";
160 INPUT PL
170 PRINT "ERROR IN CELL";
180 INPUT DPL
190 PRINT "PERCENT IMPURITY"
200 INPUT PIMP
210 T=273.15+T
220 OPEN "I",1,DFILE$
230 FOR I=1 TO 13
240 LINE INPUT #1,C$
250 PRINT C$
260 NEXT I
270 OPEN "R",2,TFILE$,18
280 FIELD #2,2 AS L$,4 AS A$,4 AS B$,4 AS S$,4 AS E$
290 IF EOF(1) THEN 520
295 INPUT #1,PT,WL
300 IF PT>=100! THEN 290
305 IF PT<=0! THEN 290
310 TRANS=100/PT
320 LNABS=LOG(TRANS)
330 AB=LNABS/2.303
340 WL%=INT(WL)
350 CONC=9.658E+18*P/T
360 SIG=LNABS/(PL*CONC)
370 ET=DT/T
380 EP=DP/P
390 EPL=DPL/PL
400 DA=.0007/AB
410  DSIG=(ET+EP+EPL+DA)*SIG
420 PRINT WL%,AB,SIG,DSIG
430 LSET L$=MKI$(WL%)
440 LSET A$=MKS$(AB)
450 LSET B$=MKS$(LNABS)
460 LSET S$=MKS$(SIG)
470 LSET E$=MKS$(DSIG)
480 WL%=WL%-184
490 PUT #2,WL%
500 IF EOF(1) THEN 520
510 GOTO 290
520 CLOSE #1
530 CLOSE#2
540 END
```

APPENDIX VI

CP/M Basic Program to Average Photoabsorption Cross-Sections

```
10 'PROGRAM TO CALCULATE THE AVERAGE CROSS SECTION
20 DEFINT I-N
30 PRINT "NUMBER OF DATA FILES TO BE AVERAGED"
40 INPUT J
45 N=J+1
50 PRINT "BEGINNING WAVELENGTH";
60 INPUT LWL
65 PRINT "ENDING WAVELENGTH";
67 INPUT NWL
70 LWL=LWL-184
75 NWL=NWL-184
80 FOR I=1 TO N
90 PRINT "FILE#";I;
100 INPUT N$
110 N$="B:"+N$
120 OPEN "R",I,N$,18
130 FIELD I,2 AS L$(I),4 AS A$(I),4 AS B$(I),4 AS S$(I),4 AS E$(I)
135 IF I<>J THEN 140
137 PRINT "DATA ";
140 NEXT I
200 FOR I=LWL TO NWL
210 AVGS=0!:AVGE=0!
220 FOR K=1 TO J
230 GET K,I
240 AVGS=AVGS+CVS(S$(K))
250 AVGE=AVGE+CVS(E$(K))
260 NEXT K
270 AVGS=AVGS/J
280 AVGE=AVGE/J
290 PRINT (I+184),AVGE,AVGS
300 LSET L$(N)=MKI$(I+184)
310 LSET S$(N)=MKS$(AVGS)
320 LSET A$(N)=MKS$(AVGE)
330 PUT N,I
340 NEXT I
350 CLOSE
360 END
```

APPENDIX VII

CP/M Basic Programs to Display Selected Cross-Section Data FIles on the Terminal or the Printer

```
5 LPRINT CHR$(30)
10 'PROGRAM TO DISPLAY CROSS SECTION DATA
20 DEFINT I-N
30 PRINT "NUMBER OF DATA FILES TO BE LISTED (MAX=5)"
40 INPUT J
50 PRINT "STATING WAVELENGTH";
55 INPUT LWL
60 PRINT "ENDING WAVELENGTH";
65 INPUT NWL
67 LWL=LWL-184:NWL=NWL-184
70 DIM L$(J),A$(J),B$(J),S$(J),E$(J)
80 FOR I=1 TO J
90 PRINT "FILE#";I;
100 INPUT N$
110 N$="B:"+N$
120 OPEN "R",I,N$,18
130 FIELD I,2 AS L$(I),4 AS A$(I),4 AS B$(I),4 AS S$(I),4 AS E$(I)
140 NEXT I
150 PRINT "FOR WHICH FILE DO YOU WISH ALL DATA DISPLAYED (# ONLY)"
160 INPUT N
170 FOR I=LWL TO NWL
180 PRINT
185 LPRINT
190 FOR K=1 TO J
200 GET K,I
210 AB=CVS(A$(K))
220 IF K>1 THEN 240
230 PRINT USING "### ";CVI(L$(K));
235 LPRINT USING "### ";CVI(L$(K));
240 IF K=N THEN 265
250 IF AB>11! THEN 300
260 IF AB<.1 THEN 300
265 IF J=1 THEN 275
270 PRINT USING "#.## ";CVS(A$(K));
271 LPRINT USING "##.## ";CVS(A$(K));
272 GOTO 280
275 PRINT USING "##.###### ";CVS(A$(K));
277 LPRINT USING "##.###### ";CVS(A$(K));
280 PRINT USING "##.###### ";CVS(S$(K));
285 LPRINT USING "##.###### ";CVS(S$(K));
290 GOTO 310
300 PRINT "                ";
305 LPRINT "                ";
310 NEXT K
320 NEXT I
330 CLOSE
340 END
```

```
10 'PROGRAM TO DISPLAY CROSS SECTION DATA
20 DEFINT I-N
30 PRINT "NUMBER OF DATA FILES TO BE LISTED (MAX=5)"
40 INPUT J
50 PRINT "STATING WAVELENGTH";
55 INPUT LWL
60 PRINT "ENDING WAVELENGTH";
65 INPUT NWL
67 LWL=LWL-184:NWL=NWL-184
70 DIM L$(J),A$(J),B$(J),S$(J),E$(J)
80 FOR I=1 TO J
90 PRINT "FILE#";I;
100 INPUT N$
110 N$="B:"+N$
120 OPEN "R",I,N$,18
130 FIELD I,2 AS L$(I),4 AS A$(I),4 AS B$(I),4 AS S$(I),4 AS E$(I)
140 NEXT I
150 PRINT "FOR WHICH FILE DO YOU WISH ALL DATA DISPLAYED (# ONLY)"
160 INPUT N
170 FOR I=LWL TO NWL
180 PRINT
190 FOR K=1 TO J
200 GET K,I
210 AB=CVS(A$(K))
220 IF K>1 THEN 240
230 PRINT USING "### ";CVI(L$(K));
240 IF K=N THEN 265
250 IF AB>1! THEN 300
260 IF AB<.1 THEN 300
265 IF J=1 THEN 275
270 PRINT USING "#.## ";CVS(A$(K));
272 GOTO 280
275 PRINT USING "##.######## ";CVS(A$(K));
280 PRINT USING "##.######## ";CVS(S$(K));
290 GOTO 310
300 PRINT "                    ";
310 NEXT K
320 NEXT I
330 CLOSE
340 END
```

APPENDIX VIII

RT-11 Basic Program to Calculate Photo-dissocition Lifetimes

```
10 REM  PROGRAM TO CALCULATE THE PHOTODISOCIATION
20 REM  RATE COEFFICIENTS GIVEN A PHOTOABSORPTION CROSS SECTION
30 REM*****************************************************
40 REM
50 PRINT "ENTER THE NAME OF OF THE CROSS SECTION DATA FILE"
60 INPUT N$
65 PRINT "ENTER THE WAVELENGTH INTERVAL OF THE DATA"
67 INPUT I1
70 PRINT "ENTER THE FINAL WAVELENGTH IN THE CROSS SECTION"
75 INPUT T
77 IF T<=539 THEN 80
78 T=539
80 OPEN N$ FOR INPUT AS FILE #1
90 OPEN "FLUX.DAT" FOR INPUT AS FILE #2
95 OPEN "LP:" FOR OUTPUT AS FILE #3
97 PRINT #3:"PHOTODISSOCIATION VALUES FOR ";N$
100 DIM S(5),F1(5),F2(5),W2(2)
110 F=.5
120 FOR I=0 TO 5\S(I)=0\NEXT I
130 REM
210 FOR I=1 TO 539
220 INPUT #1:W1,C
230 IF W1<192 THEN 220
235 IF W1<=W2(2) THEN 250
237 W2(1)=W2(2)\F1(0)=F2(0)\F1(1)=F2(1)\F1(2)=F2(2)\F1(3)=F2(3)
240 F1(4)=F2(4)\F1(5)=F2(5)
250 INPUT #2:W2(2),F2(0),F2(1),F2(2),F2(3),F2(4),F2(5)
260 IF W2(2)>W1 THEN 290
270 W2(1)=W2(2)\F1(0)=F2(0)\F1(1)=F2(1)\F1(2)=F2(2)\F1(3)=F2(3)\F1(4)=F2(4)
275 F1(5)=F2(5)
280 GO TO 250
290 IF I<T THEN 295
292 F=.5
295 FOR J=0 TO 5
300 S(J)=S(J)+F*C*(F1(J)+(F2(J)-F1(J))*(W1-W2(1))/(W2(2)-W2(1)))
320 NEXT J
322 PRINT W1,W2(1),W2(2)
323 PRINT C
325 PRINT S(0);S(1);S(2);S(3);S(4);S(5)
327 IF W1=T THEN 350
328 IF I=T THEN 350
340 NEXT I
350 FOR I=0 TO 5\S(I)=S(I)*I1\NEXT I
352 PRINT #3:"ALT (KM)","J (SEC-1)","LIFTIME (SEC)"
353 PRINT #3:0,S(0),1/S(0)
355 PRINT #3:10,S(1),1/S(1)
356 PRINT #3:20,S(2),1/S(2)
357 PRINT #3:30,S(3),1/S(3)
358 PRINT #3:40,S(4),1/S(4)
359 PRINT #3:50,S(5),1/S(5)
360 END
```

APPENDIX IX

RT-11 Basic Program to Transform Sequential ASCII Data Files to Random Access Data Files For Plottting

```
 TT:=CHANGE.BAS
10 REM PROGRAM TO CHANGE 8080 TRANSFER DATA FILE
20 REM TO LSI-11 RANDUM ACCESS DATA FILE
30 PRINT "ENTER DESIRED NEW RANDOM DATA FILE NAME "
40 INPUT N$
50 PRINT "ENTER TRANSFER DATA FILE NAME "
60 INPUT T$
70 OPEN T$ FOR INPUT AS FILE #1
80 OPEN N$ FOR OUTPUT AS FILE VF2(1000)
100 FOR I=1 TO 1000
105 IF END #1 THEN 190
110 INPUT #1:W,T
115 PRINT W,T
120 W=W-184
130 T=(INT((LOG(T)/LOG(10)+22)*100+.5))/100
140 VF2(W)=T
160 IF W=I THEN 180
170 VF2(I)=0\I=I+1\GO TO 160
180 NEXT I
190 VF2(0)=W
200 CLOSE
210 END
*
```

CP/M

```
5 DEFINT I-N
10 'PROGRAM TO CONVERT RANDOM FILE TO SEQUENTIAL
20 PRINT "NAME OF RANDOM FILE"
30 INPUT R$
35 R$="B:"+R$
40 PRINT "NAME OF SEQUENTIAL FILE TO BE BUILT"
50 INPUT N$
55 N$="B:"+N$
60 PRINT "STARTING WAVELENGTH";
70 INPUT LWL
80 PRINT "ENDING WAVELENGTH";
90 INPUT NWL
100 LWL=LWL-184:NWL=NWL-184
110 OPEN "R",1,R$,18
120 FIELD 1,2 AS L$,4 AS A$,4 AS B$,4 AS S$,4 AS E$
130 OPEN "O",2,N$
140 FOR I=LWL TO NWL
150 GET 1,I
160 L=CVI(L$)
170 S=CVS(S$)
180 PRINT L,S
190 PRINT #2,L$","S
200 NEXT I
210 PRINT #2,0
220 CLOSE
230 END
```

APPENDIX X

RT-11 Basic Program to Build Random Access Data Files for Plotting

```
 TT:=ENTRY.BAS
5 PRINT "DO YOU WISH JUST TO EXAMINE OR CHANGE DATA IN AN OLD FILE ?"
7 INPUT #0:A$
8 IF SEG$(A$,1,1)<>"Y" THEN 10
9 E=1
10 PRINT "ENTER THE DESIRED DATA FILE NAME"
20 INPUT #0:N$
40 PRINT "ENTER THE INITIAL X VALUE ";\INPUT #0:X
50 PRINT "ENTER THE X INCREMENT     ";\INPUT #0:I1
52 IF E=1 THEN 165
55 OPEN N$ FOR OUTPUT AS FILE VF1(1000)
60 PRINT " TYPE A NEGATIVE NUMBER TO EXIT,  KEEP TRACK OF ANY ERRORS"
70 I=0\J=1
80 PRINT X+I,\INPUT #0:V
90 IF V<0 THEN 120
95 V=(INT((LOG(V)/LOG(10)+22)*100+.5))/100
100 VF1(J)=V\J=J+1\I=I+I1
110 GO TO 80
120 PRINT "THERE WERE A TOTAL OF ";J-1;" POINTS ENTERED"
130 F=J-1\VF1(0)=F
135 CLOSE
140 PRINT "DO YOU WISH TO EXAMINE THE VALUES FOR ERRORS ?"
150 INPUT #0:A$
160 IF SEG$(A$,1,1)<>"Y" THEN 230
165 OPEN N$ AS FILE VF1(1000)
170 PRINT "TYPE THE NEW VALUE IF INCORRECT OR 'Y' IF CORRECT"
172 I=0
175 FOR J=1 TO VF1(0)
190 PRINT X+I,VF1(J),
195 PRINT EXP((VF1(J)-22)*LOG(10)),
197 INPUT #0:A$
200 IF SEG$(A$,1,1)="Y" THEN 220
205 V=VAL(A$)
207 V=(INT((LOG(V)/LOG(10)+22)*100+.5))/100
210 VF1(J)=V
220 I=I+I1
225 NEXT J
227 CLOSE
230 END
*
```

APPENDIX XI

RT-11 Basic Program to Plot Random Access Data Files on a 4010 Series Tektronix Terminal Equipped with a Digital Plotter

```
5 REM ************************************************
6 REM *       UV-VIS DATA PLOTTING ROUTINE            *
7 REM ************************************************
10 E$=CHR$(27)&CHR$(12)
15 O$=CHR$(4)
20 S$=CHR$(32)
25 G$=CHR$(29)
30 A$=CHR$(31)
35 U$=CHR$(14)
40 L$=CHR$(15)
45 R$=CHR$(13)
50 F$=CHR$(10)
55 B$=CHR$(8)
60 V$=CHR$(11)
65 DIM L(8)
100 REM * SET UP PLOTTING FIELD *
105 DIM C$(1023,1)
110 OPEN "GRAPH" FOR INPUT AS FILE VF1$(1023)=4
115 FOR I=0 TO 1023
120 C$(I,0)=SEG$(VF1(I),3,4)
125 C$(I,1)=SEG$(VF1(I),1,2)
130 NEXT I
135 CLOSE
200 REM * GET DATA *
205 PRINT "NAME OF DATA SET = ";\INPUT #0:N$
210 PRINT "INITIAL X = ";\INPUT #0:X1
215 PRINT "INITIAL Y = ";\INPUT #0:Y1
220 PRINT "X DATA INCREMENT = ";\INPUT #0:I1
225 PRINT "Y DATA INCREMENT = ";\INPUT #0:I2
230 PRINT "LOG OFFSET = ";\INPUT #0:O
231 PRINT " AXIS ? ";\INPUT #0:A2$
232 IF SEG$(A2$,1,1)="N" THEN 235
233 PRINT "COMPLETE AXIS ? ";\INPUT #0:A1$
235 O=O*100
250 OPEN N$ AS FILE VF1(1000)
252 N=VF1(0)
255 DEF FNZ(X2,Y2)=G$&C$(Y2,1)&C$(X2,0)
260 DEF FNP(Y2,X2,Y3,X3)=G$&C$(Y2,1)&C$(X2,0)&C$(Y3,1)&C$(X3,0)&O$
265 DEF FND(X2,Y2)=C$(Y2,1)&C$(X2,0)
300 REM * START *
305 P1=10\X=P1\Y=VF1(1)*100-(Y1*100)+10\P2=Y
310 GOSUB 1000 \REM * PLOT DATA *
312 IF SEG$(A2$,1,1)="N" THEN 355
315 P1=I1*N+P1
350 GOSUB 2000 \REM * DRAW AXIS *
355 PRINT CHR$(27)&"A"&"F"\REM PLOTTER OFF
357 PRINT FNZ(0,0)
```

```
360 ""
1000 REM ************************************************
1001 REM *              PLOTTING SUBROUTINE               *
1002 REM ************************************************
1005 PRINT CHR$(27)&"A"&"E"\REM *PLOTTER ON*
1010 FOR I=1 TO N STEP 14
1011 IF Y>10 THEN 1015
1012 IF Y<=0+10 THEN 1020
1013 S=0
1015 PRINT FNZ(X,Y);
1020 FOR J=I TO I+14
1025 IF J=N THEN 1065
1030 X=J*I1+P1\Y=VF1(J+1)*100-(Y1*100)+10
1032 IF Y<=P2 THEN 1035
1033 P2=Y
1035 IF Y<=0+10 THEN 1045
1037 IF S=1 THEN 1013
1040 PRINT FND(X,Y);
1045 NEXT J
1050 PRINT
1055 NEXT I
1060 P1=J*I1+P1
1065 PRINT
1070 RETURN
2000 REM ************************************************
2001 REM *     Y & X AXIS GENERATING SUBROUTINE          *
2002 REM ************************************************
2003 REM * DRAW BOX AROUND PLOT *
2004 PRINT FNP(10,10,P2+10,10);FNP(10,10,10,P1)
2005 IF SEG$(A1$,1,1)="N" THEN 2007
2006 PRINT FNZ(P1,10);FND(P1,P2+10);FND(10,P2+10)
2007 REM * LOG INCREMENTS *
2010 L(1)=30\L(2)=18\L(3)=12\L(4)=10\L(5)=8\L(6)=7\L(7)=5\L(8)=5
2015 P=10
2017 REM * DRAW Y AXES *
2020 FOR I=1 TO 8
2025 P=P+L(I)
2030 IF P>=P2+10 THEN 2057
2034 GOSUB 2200
2035 PRINT FNP(P,10,P,15)
2039 PRINT
2040 NEXT I
2045 P=P+5
2049 GOSUB 2200
2050 PRINT FNP(P,10,P,20)
2055 IF P<P2 THEN 2020
2057 IF SEG$(A1$,1,1)="N" THEN 2110
2065 P=10
2070 FOR I=1 TO 8
2075 P=P+L(I)
2080 IF P>=P2+10 THEN 2107
2084 GOSUB 2200
```

```
2085 PRINT FNP(P,P1,P,P1-5)
2090 NEXT I
2095 P=P+5
2099 GOSUB 2200
2100 PRINT FNP(P,P1,P,P1-10)
2105 IF P<P2 THEN 2070
2107 FOR K=1 TO 1000\NEXT K
2110 REM *NOW DRAW X AXES*
2112 C=0\Z=10\S=1
2115 FOR I=10 TO P1 STEP 100
2119 GOSUB 2200
2120 PRINT FNP(Z,I,Z+(15*S),I)
2121 GOSUB 2200
2125 FOR J=5 TO 95 STEP 10
2130 IF I+J>=P1 THEN 2155
2131 PRINT
2132 PRINT
2133 PRINT
2134 PRINT
2135 PRINT FNP(Z,I+J,Z+(5*S),I+J)
2136 IF I+J+5>=P1 THEN 2155
2137 PRINT
2138 PRINT
2139 PRINT
2140 PRINT FNP(Z,I+J+5,Z+(10*S),I+J+5)
2145 NEXT J
2147 GOSUB 2200
2150 NEXT I
2155 IF SEG$(A1$,1,1)="N" THEN 2170
2160 IF C=1 THEN 2170
2164 FOR K=1 TO 2000\NEXT K
2165 C=C+1\Z=P2+10\S=-1
2169 GO TO 2115
2170 PRINT CHR$(27)&"A"&"F"\REM *PLOTTER OFF*
2180 RETURN
2190 REM TIME DELAY SUB
2200 FOR K=1 TO 200\NEXT K
2210 RETURN
*
```

References

1. T.D. Allston, M.L. Fedyk and G.A. Takacs, J. Photochem., 1 (1978) 116; Chem. Phys. Lett., 60 (1978) 97.

2. F.S. Rowland and M.J. Molina, Geophys. Space Phys., 13 (1975) 1.

3. A.J. Illies and G.A. Takacs, J. Photochem., 6 (1976) 35.

4. L.T. Molina and J.J. Molina, Geophys. Res. Lett., 4 (1977) 83.

5. F.S. Rowland, J.E. Spencer, and J.J. Molina, J. Phys. Chem., 80 (1976) 2711.

6. L.T. Molina and M.J. Molina, J. Photochem., 11 (1979) 139.

7. (a) M.I. Dakhis, A.A. Levin and V.A. Shlyapochnikov, J. Mol. Struct., 14 (1972) 321.

   (b) M.I. Dakhis, A.A. Levin and V.A. Shlyapochnikov, J. Mol. Struct., 21 (1974) 305

8. R.F. Hampson, Chemical Kinetics and Photochemical Data Sheets for Atmospheric Reactions, Federal Aviation Administration Report No. FAA-EE-80-17, Washington, D.C. (1980)

9. R.N. Haszeldine, J. Chem. Soc., (1953) 2075.

10. B.W. Tattershall, Chem. Communications, (1970) 1522.

11. D. Marsh and J. Heicklen, J. Phys. Chem., 69 (1965) 4410.

12. M. Christie and C.J. Mathews, J. Chem. Soc. Faraday Trans. I, 72 (1976) 1652.

13. J. Jander and R.N. Haszeldine, J. Chem. Soc., (1954) 912.

14. J.B. Cumming, R. Cooper,
W.A. Mulac and S. Gordon,
Radiation Phys. Chem., 16 (1980) 207.

15. P. Gray,
Trans. Faraday Soc., 51 (1955) 1367.

16. M.J. Rossi, J.R. Barker and D.M. Golden,
J. Chem. Phys., 71 (1979) 3722.

17. (a) J.D. Park,
Chem. Abs. 62, 9010d (1965)

(b) M.M. Fein and J.E. Paustian,
Chem. Abs. 66, 77663 (1967).

18. N.N. Yarovenko and S.P. Motornyi,
J. Gen. Chem. (USSR), 30 (1960) 4029.

19. A.V. Fokin, A.T. Uzun and Y.M. Kosyrev,
J.Gen. Chem. (USSR), 36 (1966) 559.

20. B.W. Tattershall,
Chem. Communications, (1972) 1522.

21. J. Banus,
J. Chem. Soc., (1953) 3755.

22. V.A. Ginsburg, V.V. Smolyanitskaya,
A.N. Medvedev, V.S. Faermark and A.P. Tomilov,
J. Gen. Chem. (USSR), 41 (1971) 2309.

23. N.P. Ernsting and J. Pfab,
Spectrochemica Acta, A36 (1980) 75.

24. N.P. Ernsting and J. Pfab,
J. Chem. Soc., (1970) 1763.

25. J. Mason and W. von Bronswijk,
J. Chem. Soc., (1970) 1763.

26. A.P. Kudchadker, S.A. Kudchadker,
R.P. Shukla and P.R. Patnaik,
J. Phys. Chem. Ref. Data, 8 (1979) 499.

27. M.Z. El-Sabban and B.J. Zwolinski,
J. Mol. Spectrosc., 22 (1967) 23

28. K.A. Rahn, R.D. Borgs, and R.A. Duce,
Science, 192 (1976) 549.

29. C.W. Taylar, T.J. Brice and R.L. Wear,
J. Org. Chem., 5 (1966) 169.

30. D.M. Giolando, G.B. Fazekas, W.D. Taylor and G.A. Takacs, J. Photochem., 14 (1980) 335.

31. W.A. Sheppard and J.F. Harris Jr., J. Am. Chem. Soc., 81 (1960) 5106.

32. A.B. Harker, W. Ho and J.J. Ratto, Chem. Phys. Lett., 50 (1977) 394.

33. M.J. McClements and G.A. Takacs, unpublished data.

34. W.D. Taylor, T.D. Allston, M.J. Moscato, G.B. Fazekas, R. Kozlowski and G.A. Takacs, J. Chem. Kinet., 12, (1980) 231.

35. T.D. Allston, M.L. Fedyk and G.A. Takacs, Chem. Phys. Lett., 60 (1978) 97

36. A. Castelli, A. Palm and C. Alexander Jr., J. Chem. Phys., 44 (1966) 1577.

37. N.P. Ernsting, J. Pfab, J. Chem. Soc. Faraday II, 74 (1978) 2286.

38. N.P. Ernsting and J. Pfab, Chem. Phys. Lett., 67 (1979) 538.

39. R.D. Gordon and P. Luck, Chem. Phys. Lett., 65 (1979) 480.

40. R.D. Gordon, S.C. Dass, J.R. Robins, H.F. Shurevell, and R.F. Whitlock, Can. J. Chem., 54 (1976) 2658.

41. D. Forrest, B.G. Gowenlock and J. Pfab, J. Chem. Soc. Perkin II, (1978) 12.

42. J. Mason, J. Chem. Soc., (1957) 3904.

43. B.G. Gowenlock, G. Kresze, and J. Pfab, Tetrahedron Letters, (1972) 593.

44. M. Asscher, Y. Haas, M.P. Roellig and P.L. Houston, J. Chem. Phys., 72 (1980) 768.

45. P.J. Carmichael, B.G. Gowenlock and C.A.F. Johnston, J. Chem. Soc. Perkin II, (1973) 1853.

46. D.R. Stull and H. Prophet,
Project Directors,
JANAF Thermochemical Tables, 2 nd ed.,
Natl. Stand. Ref. Data Ser., Natl. Bur. Stand.,
Washington, D.C., 37 (1971).

47. J.A. Kerr and A.F. Trotmau-Dickenson,
"Strengths of Chemical Bonds",
Handbook of Chemistry and Physics, 60th ed.,
CRC Press, Inc., Bora Raton, Florida (1979-80).

48. G.D. Mendenhall, D.M. Golden, and S.W. Benson,
J. Phys. Chem., 77 (1973) 2707.

49. M.W. Chase, J.L. Curnutt, H. Prophet,
R.A. Mcdonald and A.N. Syverud,
JANAF Thermochemical Tables, 1975 Supplement,
J. Chem. Ref. Data, 4(1975) 1.

50. CODATA recommended Key Values for Thermodynamics,
1977, J. Chem. Thermodyn., 10 (1978) 903.

51. E. Kober,
J. Am. Chem. Soc., 81 (1960) 4810.

52. A.M. Basss, A.E. Ledford and A.H. Loafer,
J. Res. NBS., Vol. 80A. (1976) 143-166.